Infectious Disease Modelling 11 (2026) 896–919

Contents lists available at ScienceDirect

Infectious Disease Modelling

journal homepage: www.keaipublishing.com/idm

Modelling the effect of long-lasting insecticidal nets on malaria transmission dynamics in Kebbi State, Nigeria

Emmanuel A. Bakare [a,b,*], Idowu I. Olasupo [a,b], Micheal Imoudu [b], Afeez Abidemi [b,c], Deborah O. Daniel [b], Samuel A. Osikoya [a,b], Oluwaseun A. Mogbojuri [a,b,d], Aaron O. Nwana [b,e], Dolapo O. Oniyelu [b,f], Ronke D. Olorunfemi [b], Oluwafemi Samson Olagbami [a,b], Dorcas O. Agboola [b], Steven I. Ikediashi [b], Ayomide Adedeji [b], Oluwaponmile Ikuseka [b], Micheal Fadairo [b], Odunayo Odewale [b], Ifeoma Goodness Onwuka [b], Aurel Hansinon [b], Dolapo A. Bakare [b], Lisa J. White [i], Nakul Chitnis [j], Olusola Oresanya [k], Chukwu Okoronkwo [l], Eze Nelson [l], Segun Kosoko [a,b,g], Gabriel I. Ogban [a,b,h]

[a] Department of Mathematics, Federal University Oye-Ekiti, Nigeria
[b] International Centre for Applied Mathematical Modelling and Data Analytics, Federal University Oye-Ekiti, Nigeria
[c] Department of Mathematical Sciences, Federal University of Technology Akure, Nigeria
[d] Department of Mathematical Sciences, Adekunle Ajasin University, Akungba-Akoko, Ondo State, Nigeria
[e] Department of Animal and Environmental Biology, Parasitology Unit, Federal University Oye-Ekiti, Nigeria
[f] Department of Computer Science, Federal University Oye-Ekiti, Nigeria
[g] Department of Mathematical and Computer Sciences, University of Medical Sciences, Ondo City, Nigeria
[h] Department of Mathematics, University of Cross River State, Calabar, Nigeria
[i] Department of Biology, University of Oxford, UK
[j] Swiss Tropical and Public Health Institute, Basel, Switzerland
[k] Malaria Consortium Nigeria, Maitama, Abuja, FCT, Nigeria
[l] Surveillance, Monitoring, Evaluation and Operations Research Unit, National Malaria Elimination Programme, Abuja, Nigeria

ARTICLE INFO

Article history:
Received 22 May 2025
Received in revised form 21 January 2026
Accepted 28 January 2026
Available online 2 February 2026
Handling Editor: Dr Daihai He

Keywords:
Malaria
Long lasting insecticidal-treated nets
Insecticide-treated nets
Transmission dynamics

ABSTRACT

Background/aim: Malaria, in Nigeria, is a disease of public health concern that has caused both morbidity and mortality, with the highest prevalence in Kebbi State. Long-lasting insecticidal nets (LLINs) have been instrumental in controlling the burden of the disease. This study aims to assess the effect of LLINs on malaria transmission dynamics in Kebbi State, Nigeria.

Methods: Routine data for the confirmed uncomplicated malaria cases in Kebbi State, Nigeria, from January 2015 to May 2024 were used to understand the transmission dynamics within the population. A deterministic compartmental model was developed to capture the malaria transmission dynamics in Kebbi State. Qualitative analysis was carried out, establishing the positivity and boundedness of solutions to ensure the biological feasibility of the model. The disease-free equilibrium was analyzed for stability, revealing under which condition the disease is eradicated. Effective reproduction number, $\mathcal{R}_e$, was derived, governing the disease persistent in the presence of intervention. The endemic equilibrium was further examined to indicate situations where the disease persist in the

* Corresponding author. Department of Mathematics, Federal University Oye-Ekiti, Nigeria.
E-mail address: emmanuel.bakare@fuoye.edu.ng (E.A. Bakare).
Peer review under the responsibility of KeAi Communications Co., Ltd.

https://doi.org/10.1016/j.idm.2026.01.003

population. The model was fitted to Kebbi state monthly malaria cases using the least squares estimation method implemented in R. Numerical simulations were performed using the R software. Prediction scenarios of malaria cases considering different usage levels of LLINs (38.2%, 50% and 80%) are visualized through the simulation of the malaria model.

Results: The result showed that if there had been 80% sustained level LLINs usage as proposed by NMEP since 2015, there would have been about 5.2 million malaria cases averted, which corresponds to 97.98% reduction. However, moving forward, if 80% usage can be achieved and sustained, about 3 million malaria cases would be averted by May 2029, signifying an impressive reduction of 78.93% in incidence.

Conclusion: We conclude that in order to significantly reduce malaria incidence in Kebbi State to its bearest minimum, health policymakers and decision makers in Nigeria should prioritise scaling up LLINs distribution and usage in the state.

1. Introduction

Malaria is a disease caused by the parasite of the genus *Plasmodium* transmitted through the bite of infected female Anopheles mosquitoes (WHO; Coetzee, 2020). Five species of *Plasmodium* are known to cause malaria in humans -*Plasmodium falciparum* (*P. falciparum*), *P. vivax*, *P. ovale*, *P. malariae*, and the simian species *P. knowlesi* (WHO). Two species that pose the greatest threat are *P. falciparum* and *P. vivax* (WHO). *P. falciparum* is the most virulent species, accounting for over 97% of the total malaria cases and is the predominant species in Nigeria (WHO; Kusimo et al., 2019).Malaria is a disease of public health concern that has caused both morbidity and mortality (WHO). It remains a global health issue, with sub-Saharan Africa being the most affected region, accounting for over 90% of malaria cases and deaths (World health organization, 2021). According to the World Health Organization (WHO), 249 million malaria cases were reported globally in 2022, resulting in approximately 608,000 deaths (World health organization, 2021; World Health Organization (WHO) Africa; National Malaria Elimination Programme (NMEP), 2021a). The African continent bears a great share of this burden, with Nigeria accounting for 27% of the global malaria burden with an estimated 68 million cases and 194,000 deaths due to the disease in 2021 (World Health Organization, 2023). Also, of all the 36 States in Nigeria and the Federal Capital Territory (FCT), Kebbi State records the highest malaria prevalence with microscopy of 49% (National Malaria Elimination Programme (NMEP), 2021a; World Health Organization, 2023).

In the year 2001, Nigeria launched the National Malaria Control Program (NMCP), later renamed the National Malaria Elimination Program (NMEP), to address the burden of malaria in the country (Federal ministry of health, 2022). This was to guide the nation to achieve malaria pre-elimination and elimination as proposed in her National Malaria Elimination Strategic Plan (NMSP) (National Malaria Elimination Programme (NMEP), 2021b). Thus far, the country has successfully implemented four of her strategic plans and is currently in the fifth plan, which will elapse by the end of 2025 (Federal ministry of health, 2022; National Malaria Elimination Programme (NMEP), 2021b). Currently, major interventions such as long-lasting insecticidal nets (LLINs), case management, intermittent preventive treatment (IPTp), and seasonal malaria chemoprevention (SMC) have been deployed in Nigeria (Federal ministry of health, 2022; National Malaria Elimination Programme (NMEP), 2021b). NMEP proposes 80% scale-up of LLINs distributions in the country at 3-year intervals, owing to its proven efficacy and cost-effectiveness in reducing malaria morbidity and mortality across various regions (Adegbenro et al., 2018). However, this proposed plan has not been sustained over the years, which makes malaria remain highly endemic in the country, particularly in Kebbi State with the highest prevalence (Richards et al., 2013).

Malaria transmission in Kebbi State is seasonal, with peaks occurring during the rainy season, which usually spans from June to October (National Malaria Elimination Programme (NMEP), 2021a; Aliyu Abdulkarim et al., 2023). This period provides ideal conditions for the breeding of Anopheles mosquitoes, the primary vectors of malaria (National Malaria Elimination Programme (NMEP), 2021a; Aliyu Abdulkarim et al., 2023). Thus far, there have been three rollouts of LLINs campaigns in the State in 2009, 2014, and 2022 (National Malaria Elimination Programme (NMEP), 2021a). An estimate of 3.5 million LLINs have been distributed through mass distribution campaigns (National Malaria Elimination Programme (NMEP), 2021a; Federal ministry of health, 2022). The number of people who slept under LLINs the night before the Demographic and Health Surveys (DHS)/MIS surveys increased from 37.6% in 2015 to 38.2% in 2021 (National Malaria Elimination Programme (NMEP), 2021a; Federal ministry of health, 2022). The widespread deployment in endemic regions, particularly in Nigeria, has been instrumental in reducing the incidence and prevalence of the disease (Mehta, 2024).

Among the various aforementioned control measures, LLINs have been a major intervention in the fight against malaria in Nigeria, particularly Kebbi State (National Malaria Elimination Programme (NMEP), 2021a; Federal ministry of health, 2022). They represent a significant advancement over earlier mosquito nets, as they incorporate insecticides that repel or kill mosquitoes upon contact, thereby reducing mosquito survival and preventing bites (Bhattarai et al., 2007). Unlike

traditional insecticide-treated nets (ITNs), LLINs maintain effective insecticide levels for at least three years, even after multiple washes (Bhattarai et al., 2007; Mehta, 2024). Nevertheless, the efficacy of LLINs is often compromised by improper use. Discomfort and misconceptions about LLINs contribute to low utilization rates in some communities (Kusimo et al., 2019). Furthermore, the growing prevalence of insecticide resistance among mosquito populations poses a substantial challenge to the sustainability of LLINs as a control measure (Viana et al., 2016). This intervention has been reported to be particularly effective in high-transmission regions in Nigeria (Richards et al., 2013).

Studies have highlighted the importance of LLIN as an important and mainstay intervention against malaria in Nigeria. The work of Saleh et al. (Abubakar Saleh et al., 2018) revealed that there is a positive correlation between the use of LLINs and a decline in malaria prevalence from the 2015 MIS from across the six geopolitical zones in Nigeria (National Malaria Elimination Programme (NMEP), 2021a; Abubakar Saleh et al., 2018). Hence, there has been a recommendation to increase the distribution and access to LLINs to individuals (Abubakar Saleh et al., 2018). The study's outcome again underscores LLIN as an important intervention tool against malaria and its unwanted consequences.

Over the years, mathematical modelling has proven to be an essential tool for understanding disease transmission dynamics and informing intervention strategies (Okell et al., 2008; World Health Organization, 2010). For instance, Bakare et al. (2021) (Bakare et al., 2021) developed a mathematical model to analyse the potential impact of multiple control interventions such as educational campaigns, insecticide-treated nets, indoor residual spraying (IRS), destruction of mosquito breeding sites, treatment with artemisinin-based combination treatment (ACT) on malaria transmission in limited resources community. Gimba and Bala (2017) (Gimba & Bala, 2017) investigated the effect of bed net use, insecticide-treated nets (ITNs), temperature, and treatment on malaria transmission. The study's results showed that the mosquito biting rate peak occurs at a certain range of temperature. Also, the research findings showed that a combination of treatment and ITN's usage is the most effective intervention strategy. The study highlights that mosquito biting and death rates are the most important parameters driving malaria transmission, which suggests the effectiveness of LLINS. These results underscore the effectiveness of LLINs in reducing biting rates and increasing mosquito death rates due to the chemicals of the LLINs. Mukhtar et al. (2018) (Mukhtar et al., 2018) developed a deterministic model that captures the effect of LLINs on malaria transmission in South Sudan. The study suggests that the effective use of LLINs can reduce $\mathcal{R}_o$ and malaria transmission. It also advocates for scaling up LLIN distribution, particularly targeting households in high-risk malaria areas. Ngonghala et al. (2014) (Ngonghala et al., 2014) developed a mathematical model that represents the decrease in the effectiveness of LLINs due to physical and chemical decay and human behaviour on malaria transmission. Another work of Ngonghala (2022) (Ngonghala, 2022) studied the effects of ITNs, decay in ITNs efficacy over time, and mosquito-resistant insecticide on malaria transmission dynamics accounting for asymptomatic individuals. The findings highlight the importance of replacing ITNs before their prescribed lifespans or designing longer-lasting ITNs. Additionally, piperonyl butoxide (PBO) ITNs, which counteract insecticide resistance, are shown to be more effective than regular ITNs in controlling malaria.

Despite the reports on the effectiveness of LLINs in reducing malaria transmission, significant gaps remain in ensuring their sustained impact, particularly in regions with high malaria prevalence like Kebbi State. Challenges such as maintaining high LLIN coverage and usage, addressing insecticide resistance, and optimizing distribution strategies hinder long-term malaria control efforts. Moreover, existing studies often focus on national or sub-regional malaria trends without detailed studies on the effect of LLINs at the State level, particularly in Kebbi State. This study aims to assess the effect of LLINs on malaria transmission dynamics in Kebbi State by considering varying LLINs usage scenarios and also quantifying the number of cases averted with LLINs. This work seeks to provide evidence-based recommendations for improving malaria elimination efforts in the State.

The remaining part of the article is organized as follow. Section 2 details the materials and methods, which includes the study area, data description, model formulation methods, qualitative analysis of the model, and model calibration. Section 3 presents the results, and section 4 presents the discussion of the results. Section 5 summarizes the key findings, limitations, and direction for future studies.

2. Materials and methods

2.1. Study area

Kebbi State is a State in northwest Nigeria that lies between Zamfara and Niger State in the south and between Sokoto to the west (IDRIS, 2023; Mamoudou, 2021). The total land area of Kebbi State is around 36,800 square kilometers (Wali et al., 2022). There are two primary seasons in the State: the Rainy Season (May to October), which has the highest rainfall from July to September, and the Dry Season (November to April), which is characterized by decreased humidity and dry winds, temperatures, particularly in April, is often the warmest month (Zayyanu Magawata & Yahaya, 2019).

2.2. Data description

Monthly routine malaria data for Kebbi State from January 2015 to May 2024 was obtained from the National Malaria Data Repository (NMDR) of NMEP (National Malaria Data Repository). The data are not publicly accessible due to governmental policies to maintain confidentiality requirements, but access can be granted upon request following necessary approvals. Variables present in the data comprises of 113 observations and include confirmed uncomplicated malaria,

persons with clinically diagnosed malaria, children under 5 years who received LLIN, persons with confirmed uncomplicated malaria treated with ACT, persons clinically diagnosed with malaria treated with ACT, etc. The confirmed uncomplicated malaria cases data for Kebbi State is used in this study to understand the transmission dynamics of malaria within the population. These uncomplicated malaria cases are confirmed through the use of microscopy or rapid diagnostic tests (RDTs) for all age groups who sought care from reporting health facilities. The time series plot of the confirmed uncomplicated malaria case incidence trend is shown in Fig. 1b.

2.3. Model formulation

We develop a deterministic compartmental model that incorporates the effect of LLINs, assuming a homogeneously mixed human population across all age groups. The model is divided into two major groups: the human population and the female *Anopheles* mosquito population. The human population is subdivided into four compartments, namely, susceptible human $S_h(t)$, pre-infectious human $E_h(t)$, symptomatic infectious human $I_h(t)$, and asymptomatic infectious human $A_h(t)$. Thus, the total human population $N_h(t)$, is given as

$$N_h(t) = S_h(t) + E_h(t) + I_h(t) + A_h(t). \tag{1}$$

In our model, it is assumed that after recovery, individuals return to being susceptible. This assumption is a departure from what is seen in many malaria models in literature that move people to recovered class after recovery and thereafter to susceptible class. The latter approach has an underlying assumption that recovered individuals have anti-parasite immunity during the period they are in the recovered class, that is, individuals in the recovered class are assumed to be immune to infection, which is against the reality of *Plasmodium falciparum* malaria (Mandala et al., 2021). We acknowledge that recovery from *Plasmodium falciparum* malaria confers anti-disease immunity, that is, recovered individuals are only immune to malaria symptoms rather than the infection for some time (Mandala et al., 2021). This gives us an understanding that an individual can still be infected if exposed to infectious mosquito bites after recovery. It is known that even the anti-disease immunity is not so certain, since there is high variability in the level of this immunity among individuals, hence to simplify the complexity that may arise due to this variability, we assume that after recovery, individuals return to susceptible class.

The mosquito population is divided into three compartments; susceptible mosquitoes $S_m(t)$, pre-infectious mosquitoes $E_m(t)$, and infectious mosquitoes $I_m(t)$. The total mosquito population $N_m(t)$, is thus given as:

$$N_m(t) = S_m(t) + E_m(t) + I_m(t). \tag{2}$$

We assume a constant recruitment rate Λ_h into the susceptible human population. The susceptible human population is further increased when symptomatic infectious humans recover naturally or due to treatment at rate $\theta_I + u_2$ and become susceptible again. The population decreases when susceptible humans get infected at a rate $\lambda_h(t) = (1 - u_1)\frac{\epsilon(t)\beta_h I_m}{N_h}$, where β_h is the probability of transmission of malaria infection from an infectious mosquito to a susceptible human and $(1 - u_1)$ represents the reduction in transmission due to LLIN, with u_1, $(0 \leq u_1 < 1)$ being the protective effectiveness of LLIN.

Adapting the forcing function employed in (Bakare et al., 2020), we set the time-dependent function

$$\epsilon(t) = \epsilon_0\left(1 + b_1\cos\left(\frac{2\pi(t-\tau)}{12}\right)\right)$$

to be the seasonally-forced mosquito biting rate which accounts for the seasonal patterns observed in the data, where ϵ_0 is the per capita (baseline) biting rate of mosquitoes, b_1 is the amplitude and τ is the phase shift. The susceptible human

(a) Map of Nigeria showing Kebbi State.

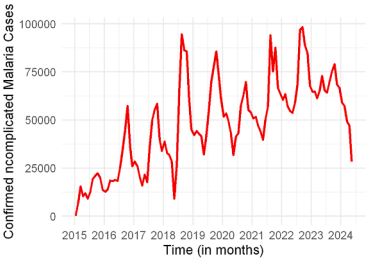

(b) Time series plot of malaria incidence in Kebbi State from January, 2015 to May, 2024.

Fig. 1. (a) Map of Nigeria showing Kebbi State. (b)Time series plot of malaria incidence in Kebbi State from January 2015 to May 2024.

population further decreases due to natural death at rate μ_h. Thus, the rate of change of the susceptible human population at any given time t is given as

$$\frac{dS_h}{dt} = \Lambda_h + (\theta_I + u_2)I_h - (\lambda_h(t) + \mu_h)S_h. \tag{3}$$

Infected humans transit to the pre-infectious class at a rate $\lambda_h(t) = (1 - u_1)\frac{\epsilon(t)\beta_h I_m}{N_h}$. At the end of the latent phase, individuals leave the pre-infectious class and become infectious at the rate σ_h. A further decrease occur in the pre-infectious human class via natural death at the rate μ_h.So, the rate of change of the pre-infectious human population is given as

$$\frac{dE_h}{dt} = \lambda_h(t)S_h - (\sigma_h + \mu_h)E_h. \tag{4}$$

The symptomatic infectious compartment is increased when a proportion ρ transit from the pre-infectious class and become symptomatic at rate σ_h. Also, the population of symptomatic infectious human is increased when asymptomatic individuals get re-infected and become symptomatic at rate $\eta\lambda_h(t)$. The symptomatic infectious class is reduced either via natural recovery or treatment-induced recovery at rates θ_I or u_2 respectively and join the susceptible class. Further reduction is due to natural death at rate μ_h and malaria-induced death at rate δ. Consequently, the rate of change of the symptomatic infectious population is given as

$$\frac{dI_h}{dt} = \rho\sigma_h E_h - (\delta + \mu_h + \theta_I + u_2)I_h. \tag{5}$$

Similarly, the asymptomatic compartment is increased when a proportion $(1 - \rho)$ moves from the exposed class and becomes asymptomatic at the rate σ_h. In this study, we assume that natural recovery from the asymptomatic state is negligible. In high-transmission settings such as Kebbi State, asymptomatic *Plasmodium falciparum* infections can persist at low parasite densities for extended periods (months or longer) in the absence of treatment (Lindblade et al., 2013; Portugal et al., 2017; Zhang & Deitsch, 2022). Frequent infectious bites in such settings have been reported to transiently increase parasite density, which may trigger the onset of symptomatic malaria (Lindblade et al., 2013). Since treatment following symptom onset constitutes the primary route of parasite clearance, and reinfection occurs on a much shorter timescale than spontaneous recovery (Ahu Prah & Laryea-Akrong, 2024), natural recovery is considered negligible for model simplification. Thus, the asymptomatic infectious population is depleted when asymptomatic individuals get re-infected and become symptomatic at rate $\eta\lambda_h(t)$, and via natural death at rate μ_h. Thus, the rate of change of the asymptomatic infectious population at time t is given as

$$\frac{dA_h}{dt} = (1-\rho)\sigma_h E_h - (\eta\lambda_h(t) + \mu_h)A_h. \tag{6}$$

Female Anopheles mosquitoes are recruited into the susceptible population at rate Λ_m. The population is reduced when susceptible female Anopheles mosquitoes get infected at a rate $\lambda_m(t) = (1 - u_1)\frac{\epsilon(t)\beta_m(\phi I_h + A_h)}{N_h}$ where, β_m is the probability of transmission from an infectious human to a susceptible mosquito and $\phi(0 < \phi < 1)$ is a modification (reduction) parameter due to reduced infectivity of symptomatic individuals compared to asymptomatic individuals. The population is further reduced due to natural death at rate μ_m. Thus, the rate of change of the susceptible mosquito population is given as

$$\frac{dS_m}{dt} = \Lambda_m - (\lambda_m(t) + \mu_m)S_m \tag{7}$$

Newly infected female Anopheles mosquitoes move to the pre-infectious class at a rate $\lambda_m(t) = (1 - u_1)\frac{\epsilon(t)\beta_m(\phi I_h + A_h)}{N_h}$. The population of pre-infectious mosquitoes decreases as they either become infectious, transitioning to the infectious class at a rate σ_m, or die naturally at a rate μ_m. So, the rate of change of the population of pre-infectious mosquitoes is given as

$$\frac{dE_m}{dt} = \lambda_m(t)S_m - (\sigma_m + \mu_m)E_m. \tag{8}$$

The infectious mosquito compartment is generated as a result of progression from the pre-infectious compartment at a rate σ_m. The population of infectious mosquitoes is decreased due to natural death at a rate μ_m. Thus, the rate of change of the population of infectious mosquito is obtained as

$$\frac{dI_m}{dt} = \sigma_m E_m - \mu_m I_m. \tag{9}$$

Table 1
Description of variables of system (10).

Variable	Description
S_h	Population of susceptible individuals
E_h	Population of pre-infectious individuals
I_h	Population of symptomatic infectious individuals
A_h	Population of asymptomatic individuals
S_m	Population of susceptible female Anopheles mosquitoes
E_m	Population of pre-infectious female Anopheles mosquitoes
I_m	Population of infectious female Anopheles mosquitoes

Table 2
Description of model parameters.

Parameter	Description
Λ_h	Recruitment rate of humans
Λ_m	Recruitment rate of mosquitoes
β_h	Transmission probability from an infectious mosquito to a susceptible human
β_m	Transmission probability from an infectious human to a susceptible mosquito
ϵ_0	Per capita (baseline) biting rate of mosquitoes
ρ	Proportion of exposed individuals progressing to the symptomatic infectious class
$1-\rho$	Proportion of exposed individuals progressing to the asymptomatic infectious class
μ_h	Per capita natural death rate of humans
μ_m	Per capita natural death rate of mosquitoes
σ_h	Progression rate exposed human class to infectious human class
σ_m	Progression rate from exposed mosquito class to the infectious mosquito class
η	Probability of asymptomatic infectious human getting more infectious bites
ϕ	Modification parameter
δ_h	Per capita disease-induced death rate for humans.
θ_I	Natural recovery rate of symptomatic individuals
u_1	Protective effectiveness of LLINs
u_2	Treatment rate
b_1	Amplitude
τ	Phase shift

From the discussion above, we obtain a seven-dimensional system of nonlinear differential equations given in equation (10). The State variables are described in Table 1 while the description of the model parameters are presented in Table 2. Fig. 2 illustrates the transmission dynamics of malaria between human and mosquito populations incorporating LLIN intervention.

$$\begin{aligned}
\frac{dS_h}{dt} &= \Lambda_h + (\theta_I + u_2)I_h - (\lambda_h(t) + \mu_h)S_h,\\
\frac{dE_h}{dt} &= \lambda_h(t)S_h - (\sigma_h + \mu_h)E_h,\\
\frac{dI_h}{dt} &= \rho\sigma_h E_h + \eta\lambda_h(t)A_h - (\delta + \mu_h + \theta_I + u_2)I_h,\\
\frac{dA_h}{dt} &= (1-\rho)\sigma_h E_h - (\eta\lambda_h(t) + \mu_h)A_h,\\
\frac{dS_m}{dt} &= \Lambda_m - (\lambda_m(t) + \mu_m)S_m,\\
\frac{dE_m}{dt} &= \lambda_m(t)S_m - (\sigma_m + \mu_m)E_m,\\
\frac{dI_m}{dt} &= \sigma_m E_m - \mu_m I_m,
\end{aligned} \tag{10}$$

with the following initial conditions:

$$S_h(0) > 0,\ E_h(0) \geq 0,\ I_h(0) > 0,\ A_h(0) \geq 0,\ S_m(0) > 0,\ E_m(0) \geq 0,\ I_m(0) > 0,$$

where

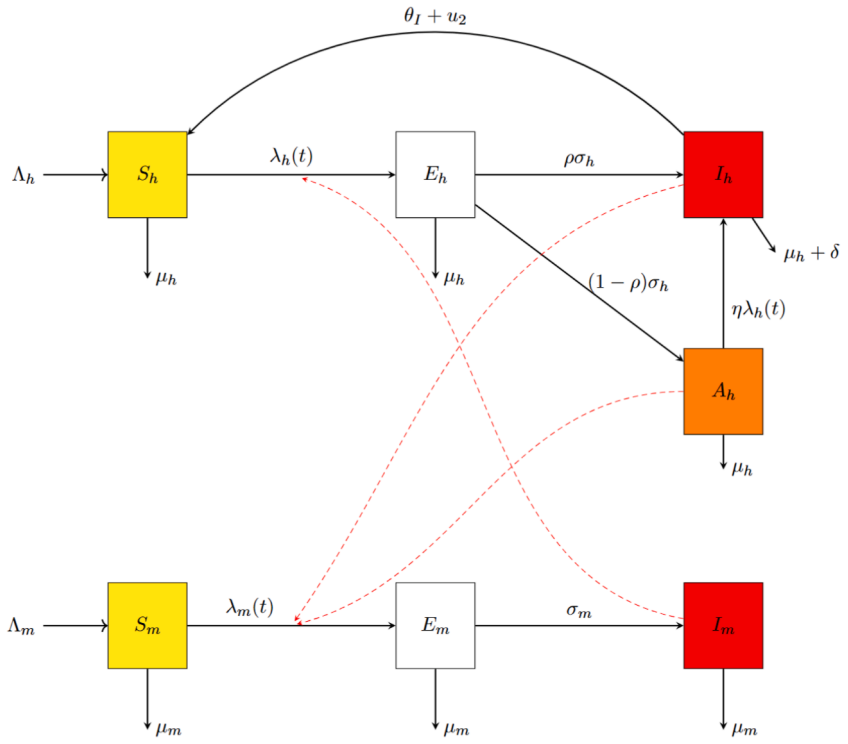

Fig. 2. The flowchart of malaria transmission dynamics between the human and mosquito population representing model (10). The black solid arrows denote transition from one compartment to another while the red dashed arrows denote disease transmission.

$$\lambda_h(t) = (1-u_1)\frac{\epsilon(t)\beta_h I_m}{N_h} \text{ and } \lambda_m(t) = (1-u_1)\frac{\epsilon(t)\beta_m(\phi I_h + A_h)}{N_h}.$$

2.4. Model analysis

This part of the paper focuses on the qualitative analysis of the autonomous version of the malaria model (10). Specifically, the analysis addresses the boundedness and positivity of solutions, the existence of equilibria, the local stability of the disease-free equilibrium, and local sensitivity analysis. Refer to A for detailed results of the analysis.

2.5. Model calibration

This section presents the calibration process for system (10). Kebbi State monthly malaria cases from 2015 to 2024 were used to calibrate model (10) using the method of least squares estimate with R software. The method seeks to find the model parameter values that minimise the sum of squared errors between the model and the data, that is

$$\min_{\theta}\left(\sum_{i=1}^{n}(y_i - \widehat{y}_i(x,\theta))^2\right),$$

where y_i is the number of malaria cases at the ith month and $\widehat{y}_i(x,\theta)$ is the estimated malaria cases at the ith month which depend on the model State variable x and parameter θ.

The initial conditions for malaria model (10) are obtained as follows: The symptomatic infectious human population is taken to be the number of cases in January 2015, hence $I_h(0) = 177$. We assume that the exposed human population $E_h(0) = 0$. Asymptomatic infectious humans is assumed to be 5 times as much as $I_h(0)$, that is $A_h(0) = 5 \times I_h(0) = 885$. The total human population of Kebbi State in 2015 was 4, 377, 770, so that the initial total human population is taken as $N_h(0) = 4, 377, 770$. It follows that the initial susceptible human population is obtained as $S_h(0) = N_h(0) - (E_h(0) + I_h(0) + A_h(0)) = 4, 377, 770 - (177 + 885) = 4, 376, 708$.

For the mosquito population, we assume that the initial total mosquito population is 5 times the total human population, that is, $N_m(0) = 5 \times N_h(0) = 21, 888, 850$. The initial size of the exposed mosquito population is assumed to be $E_m(0) = 0$,

while the initial infected mosquito population is taken as $I_m(0) = 200,000$. Consequently, the initial susceptible mosquito population is obtained as $S_m(0) = 5 \times 4,377,770 - 200,000 = 21,688,850$.

The model's parameters are estimated via the calibration process except for the recruitment rate of humans Λ_h, the recruitment rate of mosquito Λ_m, natural death rate of humans and mosquitoes μ_h and μ_m respectively, and recovery rate for symptomatic humans θ_I. The parameters μ_h and μ_m are calculated as the inverse of the average human lifespan in Kebbi State and life span of mosquito respectively, so that $\mu_h = \frac{1}{L_h} = \frac{1}{60.5 \times 12} = 0.001377$ per month, where $L_h = 60.5 \times 12$ represents the average human lifespan in Kebbi State (in months) (National population commission, 2018). and $\mu_m = \frac{1}{L_m} = \frac{30}{14} = 2.1428$ per month, where $L_m = 14/30$ represents the average lifespan of a mosquito (in months) (CDC, 2024). The parameters Λ_h and Λ_m are calculated as follows: since the total population of Kebbi State is 4, 377, 770 in 2015, then, $\Lambda_h = \frac{1}{L_h} \times 4,377,770 = 6028.18$, and $\Lambda_m = \frac{1}{L_m} \times 5(4,377,770)$. The recovery rate for symptomatic individuals is calculated by taking the inverse of its average infectious period, $\theta_I = \frac{1}{9.5}$ per month (Chitnis et al., 2008). The progression rate of the exposed human class to the infectious human class and from the exposed mosquito class to the infectious mosquito class (σ_h and σ_m) is obtained by the inverse of the average incubation period of *P. falciparum* parasite in humans and mosquitoes, $\sigma_h = \frac{1}{10/30} = 3$ per month, $\sigma_m = \frac{1}{10/30} = 3$ per month (Chitnis et al., 2008). Protective effectiveness of LLINs, u_1, is considered as a product of LLIN efficacy and LLIN usage (i.e. LLIN efficacy $\times$ LLIN usage). According to (Obi et al., 2020; WHO, 2005), a newly acquired LLIN is expected to have an efficacy between 0.9 and 1. Thus, we set the LLIN efficacy as 0.9 in this study. The baseline LLIN usage is 0.382 (National Malaria Elimination Programme (NMEP), 2021a). Consequently, the protective effectiveness of LLINs is calculated as $u_1 = 0.9 \times 0.382 = 0.3438$. In addition, the efficacy of ACT is reported to be 0.98 (National Malaria Elimination Programme (NMEP), 2021a). The treatment coverage (that is, proportion of confirmed uncomplicated malaria cases treated with ACT) is obtained from the data as 0.99. Based on therapeutic efficacy studies (Ojurongbe et al., 2013), it is expected that gametocyte clearance occurs within 3–28 days of ACT use. The treatment rate due to ACT, u_2, is therefore obtained using the survival function to convert from proportion to rate as $-\frac{\log_e(1-0.99\times0.98)}{28} \times 30 = 3.764$ per month. The remaining parameters β_h, β_m, ρ, η, τ and b_1 are obtained using the least-square curve fitting method implemented in R programming.

As a measure of the goodness-of-fit, the index of agreement (IOA) is used to quantify the agreement between model (10) and Kebbi State monthly malaria cases presented in 1b. The IOA is a widely used statistical metric for evaluating the performance of predictive models, particularly in environmental modelling contexts (Legates & McCabe, 1999). It quantifies how well model prediction matches observed data, considering both the magnitude and direction of deviations (Legates & McCabe, 1999; Willmott, 1981). The IOA originally proposed by Willmott (Willmott, 1981) is mathematically expressed as

$$\mathrm{IOA} = 1 - \frac{\sum_{i=1}^{n} (y_i - \widehat{y}_i)^2}{\sum_{i=1}^{n} (|\widehat{y}_i - \overline{y_i}| + |y_i - \overline{y_i}|)^2},$$

where y_i is the reported malaria cases, $\widehat{y}_i$ is the predicted values from the model (10), $\overline{y_i}$ is the mean of reported malaria cases and $i = 1, \ldots, n$ (n is the number of observations). The value of IOA lies between 0 and 1, with 0 indicating no agreement and 1 indicating perfect agreement between the model and the data.

2.6. Numerical simulations

Numerical simulations were performed using the estimated parameters obtained from the model calibration described in Subsection 2.5, together with the fixed parameter values listed in Table 3 and the specified initial conditions for Kebbi State. The initial conditions were defined to represent the all-age population of Kebbi State, thereby enabling simulation of the disease dynamics for the entire human population.

Local sensitivity analysis was performed to determine the parameters that are influential on the effective reproduction number, $\mathcal{R}_e$. The variations of the effective reproduction number and malaria prevalence with respect to the identified key parameters were assessed using heatmaps. These visualisations enable the systematic assessment of how changes in parameter values influence malaria transmission dynamics.

The calibrated deterministic model was solved numerically to generate monthly malaria incidence trajectories under alternative LLIN use scenarios. Simulations were performed over two time horizons. First, a retrospective simulation covering the fitted observation period (January 2015–May 2024) was used to evaluate the counterfactual effects of varying LLIN use on malaria transmission dynamics. This retrospective analysis quantified the magnitude of malaria cases that could have been averted relative to the baseline LLIN use of 38.2%, which corresponds to an estimated LLIN protective effectiveness of $u_1 = 0.34$. Alternative scenarios assumed increased LLIN use of 50% and 80%, corresponding to protective effectiveness values of $u_1 = 0.45$ and $u_1 = 0.72$, respectively. These scenarios are based on the assumption that the protective effectiveness remains constant throughout the studied period.

Second, simulations of future monthly malaria incidence were conducted under the 50% and 80% LLIN use scenarios to assess their potential long-term influence on malaria transmission in Kebbi State. These prospective simulations assumed

Table 3
Parameter values for the malaria transmission model (10).

Parameter	Value	Unit	Source
β_h	0.13044	Dimensionless	Fitted
β_m	0.01000	Dimensionless	Fitted
μ_h	0.00137	Per month	National population commission (2018)
μ_m	2.1428	Per month	Chitnis et al. (2008)
ρ	$\frac{1}{6}$	Dimensionless	Fitted
σ_h	3	Per month	Chitnis et al. (2008)
σ_m	3	Per month	Chitnis et al. (2008)
θ_l	$\frac{1}{9.5}$	Per month	Chitnis et al. (2008)
η	0.07973	Per month	Fitted
δ	2.7×10^{-3}	Per month	Chitnis et al. (2008)
Λ_h	6028.18	Per human per month	Derived
Λ_m	45966585	Per mosquito per month	Derived
ϕ	0.7	Dimensionless	Assumed
u_1	0.3438	Dimensionless	(National Malaria Elimination Programme (NMEP), 2021a)
u_2	3.764	Dimensionless	Chitnis et al. (2008)
τ	8.68604	Dimensionless	Fitted
b_1	0.16400	Dimensionless	Fitted
ϵ_0	13	Per month	Chitnis et al. (2008)

that other intervention components and demographic parameters remained constant, thereby isolating the effect of increased LLIN use.

From a policy perspective, the 50% LLIN use scenario reflects a moderate but realistic improvement achievable through sustained routine distribution and community engagement, while the 80% scenario represents an aspirational but programmatically relevant target aligned with intensified mass distribution campaigns and improved net retention and usage. Together, these scenarios provide quantitative evidence to inform LLIN scale-up strategies and highlight the potential public health gains from translating LLIN ownership into consistent and effective use across communities in Kebbi State.

3. Results

This section reports the analytical and numerical results of the malaria model (10).

3.1. Analytical results for the autonomous version of the model

According to the results of the qualitative analysis of the malaria model (10) in A, the malaria model is shown to be well posed and biologically meaningful, as both the human and mosquito populations remain uniformly bounded and all state variables remain non-negative for all time. The model admits a unique disease-free equilibrium (DFE), where the human and mosquito populations settle at their respective demographic steady states in the absence of infection. Also, an explicit expression for the effective reproduction number $\mathcal{R}_e$ is derived using the next-generation approach. The DFE is locally asymptotically stable when $\mathcal{R}_e < 1$ and becomes unstable when $\mathcal{R}_e > 1$, establishing $\mathcal{R}_e$ as the threshold parameter governing malaria transmission.

The model further admits endemic equilibria, whose number depends on parameter combinations and the value of $\mathcal{R}_e$. In particular, a unique endemic equilibrium exists when $\mathcal{R}_e > 1$, while multiple endemic equilibria may occur, including the possibility of endemic equilibria when $\mathcal{R}_e < 1$, indicating the potential for backward bifurcation.

Moreover, the analytical results from the sensitivity analysis reveal that mosquito biting rate and transmission probabilities are among the key parameters with positive signs, such that the effective reproduction number, $\mathcal{R}_e$, will increase when their baseline values are increased, and decrease when their baseline values are decreased. Conversely, control-related parameters, particularly LLIN protective effectiveness and treatment rate, are part of the model parameters having negative sensitivity indices. The effective reproduction number, $\mathcal{R}_e$, will increase when their baseline values are decreased and vice-versa highlighting their critical role in malaria control.

3.2. Model fit quality

The result of fitting the model equation (10) with the actual Kebbi State malaria incidence data is displayed in Fig. 3, while Table 3 gives the summary of the model parameter values obtained from the fitting process. The IOA is 0.9308, which implies a strong degree of agreement between the model and the data.

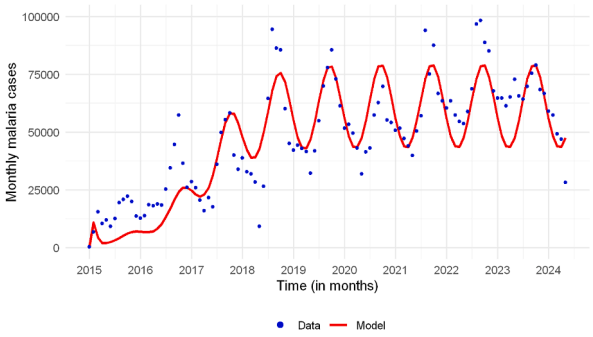

Fig. 3. Plot showing monthly observed malaria cases in Kebbi State (dots) compared with the model-based fitted output from model (10) (solid line), illustrating the model's ability to capture the temporal dynamics of malaria incidence.

3.3. Quantitative outcome of local sensitivity analysis

In Table 4, the sensitivity indices of the effective reproductive number, $\mathcal{R}_e$, with respect to the model parameters, using the baseline values of the parameters in Table 3, are presented. It is observed from Table 4 that the model parameters are categorised into two according to the signs of their sensitivity indices – those that have positive sign of sensitivity index (ϵ_0, β_h, σ_h, ϕ, ρ, β_m, σ_m, Λ_m) and those that have negative sensitivity index (μ_h, δ, θ_l, Λ_h, μ_m, u_1, u_2). The most sensitive parameters in the first category are ϵ_0, β_h, β_m and Λ_m, while the most sensitive parameters in the second category are μ_m, u_1 and Λ_h. The parameters with positive sensitivity index imply that the value of the effective reproduction number, $\mathcal{R}_e$, will increase (or decrease) when the value of any of the parameters in this category is increased (or decreased). For example, the normalized sensitivity index of $\mathcal{R}_e$ with respect to ϵ_0, $\Theta_{\epsilon_0}^{\mathcal{R}_e} = +1$ suggests that the value of the effective reproduction number, $\mathcal{R}_e$, will increase by 10% when the value of the per capita biting rate of mosquitoes, ϵ_0, increases by 10%. Similarly, the negative sign of the effective reproduction number, $\mathcal{R}_e$ to the model parameters suggests that an increase in the value of any of the parameters in this category will lead to a decrease in $\mathcal{R}_e$ value. For example, $\Theta_{\mu_m}^{\mathcal{R}_e} = -1.2083$ suggests that 10% increase (or decrease) in the baseline value of the natural mortality rate of mosquitoes, μ_m, corresponds to 12.083% decrease in the value of $\mathcal{R}_e$. We further focus on the most sensitive model parameters - per capita mosquito biting rate (ϵ_0), protective effectiveness of LLINs (u_1), transmission probabilities in human and mosquito populations (β_h and β_m, respectively) and natural mortality rate of mosquitoes (μ_m) - and numerically illustrate how they influence the dynamics of malaria transmission. See the results in Figs. 4 and 5.

The plots in Fig. 4 demonstrate how variations in the most sensitive parameters—the per capita mosquito biting rate (ϵ_0), mosquito natural mortality rate (μ_m), transmission probability from an infectious mosquito to a susceptible human (β_h), and transmission probability from an infectious human to a susceptible mosquito (β_m)—affect the effective reproduction number ($\mathcal{R}_e$). High $\mathcal{R}_e$ values are observed in regions with weak control and high transmission, whereas low values occur when the protective effectiveness of LLINs (u_1) is sufficiently large, shifting the system toward the disease-free region. The red contour corresponding to $\mathcal{R}_e = 1$ demarcates the threshold between sustained transmission and potential disease elimination. Notably, the steep transition around this threshold suggests that modest changes in LLIN protective effectiveness near critical levels can significantly alter $\mathcal{R}_e$ to drop below one.

The incidence heatmap in Fig. 5 exhibits trends consistent with the reproduction number analysis above. Total cases increase sharply with higher mosquito biting rates (ϵ_0) and with increasing transmission probabilities in humans and mosquitoes (β_h and β_m), reaching peak values under high transmission intensity (Fig. 5a–s c and d). In contrast, total cases decline markedly with increasing mosquito natural mortality (μ_m) and higher protective effectiveness of LLINs (u_1), as shown in Fig. 5b, c, and 5d. The steep gradient from high (yellow) to low (blue) incidence indicates strong sensitivity of disease burden to these parameters.

Table 4
Sensitivity indexes of the effective reproduction number, $\mathcal{R}_e$, to the parameters of malaria model (10).

Parameter	Sensitivity index	Parameter	Sensitivity index
ϵ_0	$+1$	θ_l	-9.4300×10^{-7}
β_h	$+0.50$	β_m	$+0.50$
μ_h	-1.93542×10^{-4}	σ_m	$+0.2083$
σ_h	$+0.00023$	Λ_m	$+0.50$
ϕ	$+0.00002476$	Λ_h	-0.50
ρ	$+0.00003470$	μ_m	-1.2083
u_1	-0.5239	δ	-1.7258×10^{-8}
u_2	-3.372×10^{-5}		

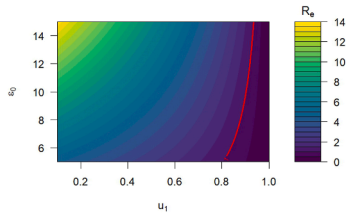

(a) Variation of the effective reproduction number, $\mathcal{R}_e$, as a function of the biting rate of mosquitoes, ϵ_0, and the protective effectiveness of LLINs, u_1

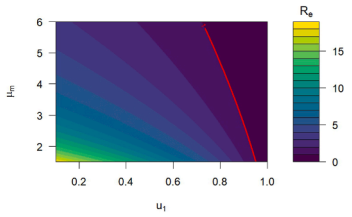

(b) Variation of the effective reproduction number, $\mathcal{R}_e$, as a function of the natural death rate of mosquitoes, μ_m, and the protective effectiveness of LLINs, u_1

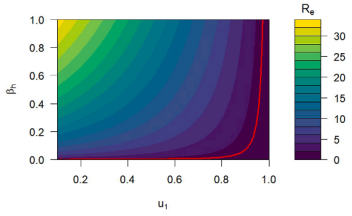

(c) Variation of the effective reproduction number, $\mathcal{R}_e$, as a function of the transmission probability from an infectious mosquito to a susceptible human, β_h, and the protective effectiveness of LLINs, u_1

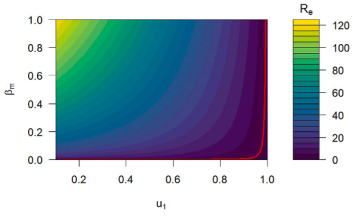

(d) Variation of the effective reproduction number, $\mathcal{R}_e$, as a function of the transmission probability from an infectious human to a susceptible mosquito, β_m, and the protective effectiveness of LLINs, u_1

Fig. 4. Heat map showing the variations of the effective reproduction number, $\mathcal{R}_e$ with respect to different combinations of key sensitive parameters with the protective effectiveness of LLINs (u_1). The colour gradient represents the magnitude of $\mathcal{R}_e$, while the red contour line denotes the epidemic threshold ($\mathcal{R}_e = 1$), separating regions of disease persistence ($\mathcal{R}_e > 1$) from elimination ($\mathcal{R}_e < 1$)

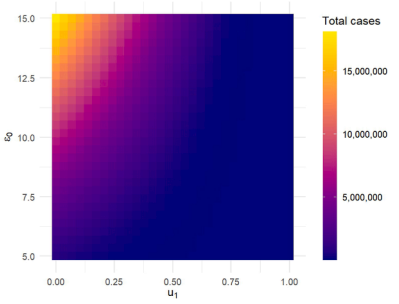

(a) Variation in total infection cases as a function of the biting rate of mosquitoes, ϵ_0, and the protective effectiveness of LLINs, u_1

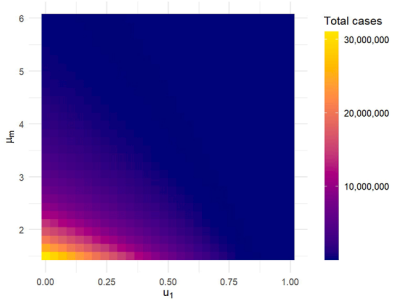

(b) Variation in total infection cases as a function of the natural death rate of mosquitoes, μ_m, and the protective effectiveness of LLINs, u_1

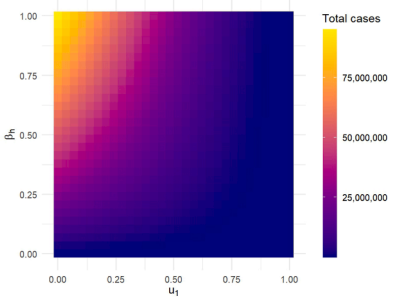

(c) Variation in total infection cases as a function of the transmission probability from an infectious mosquito to a susceptible human, β_h, and the protective effectiveness of LLINs, u_1

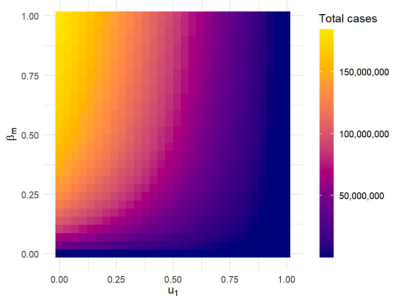

(d) Variation in total infection cases as a function of the transmission probability from an infectious human to a susceptible mosquito, β_m, and the protective effectiveness of LLINs, u_1

Fig. 5. Heat map showing the variations in total infection cases with respect to different combinations of key sensitive parameters with the protective effectiveness of LLINs (u_1). The color gradient represents total cumulative cases.

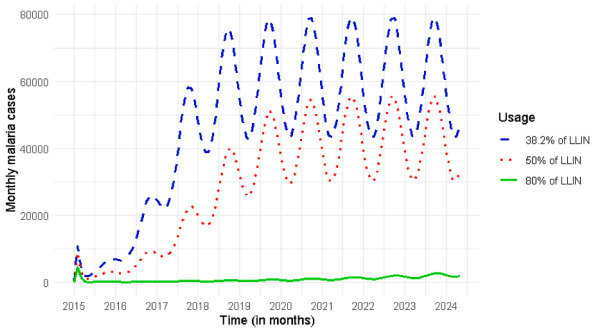

Fig. 6. Simulated malaria case trajectories in Kebbi State, Nigeria, under alternative long-lasting insecticidal net (LLIN) usage scenarios. The trajectories illustrate the influence of varying LLIN coverage on malaria transmission dynamics: the dashed blue line represents the baseline LLIN usage of 38.2%, the broken red line represents 50% LLIN usage, and the solid green line represents 80% LLIN usage.

3.4. Retrospective assessment of the effect of LLINs on malaria incidence

To assess the effects of LLIN on malaria transmission in Kebbi State, numerical simulations of the monthly malaria incidence were performed. Fig. 6 shows the simulated monthly incidence of malaria in Kebbi State for a period of 13 months (January 2015 to May 2024) with three different levels of LLIN usage: 38.2%, 50%, and 80%. This illustrates the potential evolution of malaria transmission under these different scenarios. This is based on the assumption that each level of coverage remains constant throughout the studied period, allowing for a retrospective assessment of the situation regarding malaria transmission at these levels. The baseline usage of LLIN is 38.2% obtained from the National Malaria Indicator Survey (NMIS).

Fig. 6 provides information on how variation in LLIN usage between January 2015 and May 2024 could have reduced malaria incidence cases in Kebbi State. By comparing these scenarios at 50%, and 80% levels of usage, we can better understand the role of LLIN in reducing malaria transmission in Kebbi State. The blue line represents the baseline scenario with 38.2% LLIN usage; meanwhile, NMEP proposed increasing their coverage level (same as usage in the context of this paper) to 80% by 2025 (National Malaria Elimination Programme (NMEP), 2021b). These figures formed the choice of usage level adopted for simulation for this study.

The red line, which corresponds to 50% LLIN usage, shows a decrease in malaria incidence compared to the baseline. In this scenario, the incidence of malaria cases remains high throughout the period, indicating that with low usage, a large percentage of the population remains unprotected, allowing continuous mosquito-human transmission due to the limited impact of LLIN usage. This implies that, by increasing usage by only 11.8%, the number of malaria cases reduced with an estimated 1,980,288 cases averted, equating to a 37.89% reduction relative to the 38.2% usage level.

3.5. Prospective assessment of the effect of LLINs on malaria incidence

In addition, the result in Fig. 7 illustrates the prediction of malaria incidence in Kebbi State from June 2024 to December 2029, with respect to different scenarios under consideration. Before this point, malaria incidence followed a historical trajectory, represented by the blue plot in Fig. 7, which reflects a “business as usual” scenario with a baseline LLIN usage of 38.2%. After May 2024, we implemented two additional LLIN usage levels: 50% and 80%. By integrating these different usage levels into our model, we simulated their effects on malaria incidence and visualized the results alongside the historical

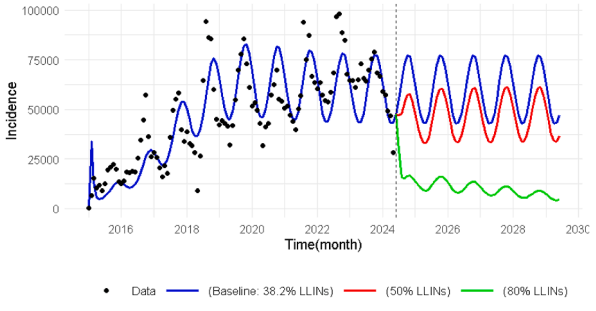

Fig. 7. Model-based prediction of malaria cases in Kebbi State, Nigeria, from June 2024 to December 2029 under varying levels of LLIN usage. Dots represent observed data, while solid lines denote scenario-based predictions: blue indicates the baseline LLIN usage of 38.2%, red represents 50% LLIN usage, and green represents 80% LLIN usage.

Table 5
Results of the estimated number of averted malaria cases under different usage levels of LLINs relative to the baseline usage.

Scenarios	Usage level of LLINs	Relative cases averted	Percentage case averted(%)
A	50%	1,980,288	37.89
B	80%	5,121,122	97.98

data, represented by black dots. This allowed us to effectively compare the actual observed incidence with our model predictions.

In order to quantify the impact of these increased LLIN usage levels, we calculated the total predicted incidence for each scenario. The findings revealed that with a baseline usage of 38.2%, the predicted incidence was approximately 3,681,628 cases as displayed in Table 6. In contrast, with a 50% usage level, the incidence decreased to about 2,643,205 cases, while an 80% usage level led to a further reduction to approximately 775,551 cases. According to the analysis, a 50% increase in usage is predicted to avert approximately 1,038,423 malaria cases, corresponding to a 28.21% reduction in predicted incidence. Moreover, scaling up usage to 80% could avert about 2,906,077 cases, signifying an impressive reduction of 78.93% in incidence (see Table 6).

4. Discussion

In this section, a detailed discussion of the results is considered. The results of the local sensitivity analysis, summarised in Table 4 offer insightful information about how the protective effectiveness of LLINs, u_1, influences the transmission dynamics and control of malaria in the interacting populations of human and mosquito. In particular, a 10% increase in the protective effectiveness of LLINs will lead to approximately a 5% reduction in the effective reproduction number. Therefore, intensifying the efforts on LLINs usage may be helpful towards malaria elimination in the population.

The results arising from the effective reproduction number heatmap highlight the importance of LLINs in mitigating malaria transmission. Even modest improvements in u_1 near the critical threshold can effectively drive $\mathcal{R}_e$ below one, promoting disease elimination. Maintaining high protective effectiveness of LLINs can offset moderate to high transmission potential and reduce the risk of resurgence, emphasising the need for sustained vector control interventions to ensure long-term suppression of malaria spread. Furthermore, the results of the incidence heatmap highlight the effectiveness of LLINs in reducing malaria incidence, even in settings with elevated transmission potential like Kebbi State. The sharp transitions observed in the heatmaps suggest that moderate increases in LLIN protective effectiveness can lead to substantial reductions in total cases. This underscores the importance of sustained LLIN usage and reinforces the role of vector control interventions in mitigating disease burden and preventing malaria resurgence.

This outcome shows the benefit of moderate improvements in LLIN usage, illustrating scaling LLIN usage to half of the population could achieve 37.89% malaria cases averted in Kebbi State (see Table 5). This level of reduction emphasises improvement achievable through intermediate LLIN usage goals, especially in settings where full LLIN adoption may be challenging to implement immediately. The green line, which represents the plot of the highest usage level at 80%, demonstrates the most dramatic effect of LLIN on malaria incidence. At this usage level, malaria cases decrease rapidly over the period, nearing elimination in the latter years. Compared to the baseline, 80% LLIN usage is expected to avert 5,121,122 malaria cases, amounting to a 97.98% reduction in malaria cases, as seen in Table 5. This finding shows the potential effect of high usage in effectively reducing malaria transmission, suggesting that malaria could be brought under control within a decade if a sustained 80% usage level is achieved and maintained. Such significant reduction provides compelling evidence that high LLIN usage could serve as a basic strategy for malaria elimination in Kebbi State and similar endemic regions, provided other malaria control interventions are maintained.

The retrospective (2015–2024) and prospective (2024–2029) simulations, conducted by maintaining fixed LLIN usage scenarios in the calibrated model, highlight a clear dose-response relationship: even moderate increases from the baseline 38.2% (NMIS-derived) yield substantial averted cases (37.89% historically at 50%, 28.21% projected forward), while the NMEP target of 80% usage drives malaria cases to near-elimination. In the context of Kebbi State's ongoing high incidence despite past distribution efforts (World Health Organization Regional Office for Africa, 2023), these numerical outcomes underscore high LLIN usage as a high-impact intervention with profound public health implications, which potentially averts millions of cases and, by extension, reduces morbidity and mortality.

These findings align with the results reported by some previous studies (Kumar et al., 2020; Mosha et al., 2022; UNICEF, 2022; Wubishet et al., 2021), supporting the effectiveness of LLINs in reducing malaria incidence. For instance, the study in (UNICEF, 2022) revealed that the use of LLIN led to a 50% reduction in malaria incidence in sub-Saharan Africa. Consequently, these results align with global malaria control strategies endorsed by WHO (World Health Organization, 2023), which recommended scaling up the distribution of LLIN and other preventive measures in high-burden settings (World Health Organization, 2017). This paper supports the United Nations' Sustainable Development Goal 3 (SDG 3), which seeks to ensure healthy lives and promote well-being for all. In particular, we focus on target 3.3, which aims to eliminate malaria and other diseases by 2030. In line with SDG 3, this study contributes to current malaria control efforts and will help to improve the distribution of LLINs in Kebbi State.

Table 6
Results of the estimated number of averted malaria cases for 5 years prediction under different usage levels of LLINs relative to the baseline usage.

Scenarios	usage level of LLINs	Total cases	Relative cases averted	Percentage case averted(%)
Baseline	38.2%	3,681,628	–	–
A	50%	2,643,205	1,038,423	28.21
B	80%	775,551	2,906,077	78.93

Our findings reveal that while LLIN usage is currently at 38.2%, malaria cases remain high, a clear indication that many individuals are either not receiving nets or, more critically, not using them consistently. To effectively reduce malaria transmission in Kebbi State, public health policymakers must urgently refocus efforts on increasing the actual usage of LLINs, not merely their distribution. The implications of our results for public health policy in Kebbi State highlight that increasing LLIN usage not only protects more people but also helps kill mosquitoes, reducing their lifespan and ability to transmit the disease. This explains the trends we see in our simulation results and point to clear actions: reduce mosquito bites through prevention, increase mosquito death rates through vector control, and expand LLIN usage as widely as possible.

The result also offers practical insights for planning and resource allocation. Reaching 50% LLIN usage is a realistic short-term goal that can still make a big difference, especially in areas with limited resources. Achieving 50% usage represents a feasible intermediate target through targeted mass campaigns, continuous distribution via antenatal clinics and schools, and community engagement in resource-limited settings (Babalola et al., 2019). This aligns with ongoing efforts in Nigeria, where moderate scale-up has shown impact despite challenges (Dako-Gyeke et al., 2024).

In the long term, aiming for 80% usage – consistent with NMSP 2021–2025 targets for at least 80% access and utilization of key vector control interventions – should be a top priority (National Malaria Elimination Programme (NMEP), 2021b). Reaching and sustaining this level requires a multi-pronged realistic approach: intensified mass distribution campaigns, routine replacement of expired or damaged nets, and sustained behaviour change communication. These national efforts on LLIN implementation in high-burden states like Kebbi, could accelerate progress toward the NMSP goal of <10% parasite prevalence by 2025 with extended ambitions toward 2030 elimination.

While the simulations assume constant coverage and no major shifts in other interventions, they provide robust projections under these conditions, underscoring the need for complementary strategies (e.g., resistance monitoring, larval source management) to realize full benefits in real-world settings. Even modest improvements in usage can yield dramatic health benefits. These predictions reinforce the importance of LLINs as a frontline tool in Nigeria's malaria elimination strategy.

Although LLIN distribution campaigns have been implemented in the past, there is a pressing need to assess whether these nets are being used effectively. Mass replacement of expired or damaged LLINs should be prioritized, especially in communities where usage has declined due to wear and tear or misconceptions. Distribution efforts must be paired with planned follow-up mechanisms to ensure that nets are not only delivered but also installed and used correctly. Community health workers should be trained and deployed to conduct household visits, demonstrate proper net hanging techniques, and monitor usage patterns over time.

Equally important is addressing the behavioural and cultural barriers that hinder LLIN usage. Many individuals avoid using nets due to discomfort, heat, or unfounded fears (National Malaria Elimination Programme (NMEP), 2021a). To overcome these challenges, literacy and orientation campaigns must be intensified. These should be delivered in local languages and tailored to community norms, using trusted voices such as religious leaders, traditional rulers, and local influencers. Radio programs, street theatre, and mobile messaging can be powerful tools to normalise LLIN usage and dispel myths. Where such efforts are already in place, they must be sustained and scaled; where absent, they should be urgently introduced.

Despite the progress that could be made due to the use of LLINs, as the findings of this study have revealed, potential barriers such as inconsistent use of nets, mosquitoes developing resistance to insecticides, and difficulties in getting nets to remote communities can limit the success of LLIN in preventing malaria incidence in Kebbi State. Addressing these issues is essential to fully achieve the benefits shown in our results.

Finally, policymakers must invest in monitoring and evaluation systems that track not just LLIN usage, but actual usage rates and their impact on malaria incidence. Real-time data dashboards, periodic household surveys, and community feedback loops are essential for refining strategies and ensuring accountability. Continued political commitment, adequate funding, and community ownership will be vital to sustaining progress. The evidence is clear: increasing LLIN usage, not just usage, is the key to unlocking major health gains and moving Kebbi State closer to malaria elimination. With the right investments and strategies, Kebbi State can make major progress toward eliminating malaria.

5. Conclusion

Long-lasting insecticidal nets (LLINs) are a major control intervention tools for the fight against malaria in Nigeria. In this study, a deterministic compartmental model of malaria that incorporates the effects of LLINs was fitted to the monthly routine data for Kebbi State, Nigeria from January 2015 to May 2024. To establish the epidemiological feasibility of the

malaria model, we performed some qualitative analysis such as positivity and boundedness of solutions. The effective reproduction number was computed, and the stability of equilibria under certain conditions was analyzed. Model fitting and parameter estimation were performed using the least squares method. Some of the parameters were obtained from existing literature while others were derived from demographic data. The effective reproduction number $\mathcal{R}_e$ was estimated to be 7.39.

Local sensitivity analysis was performed to determine the most influential parameters driving malaria transmission in Kebbi State. The study showed that in comparison to the baseline usage, 50% LLIN usage will lead to reduction of malaria cases by 37.89% while 80% LLIN usage will reduce malaria cases by 97.98%. We also carried out scenario analysis to make a 5-year prediction of malaria incidence with varying levels of LLINs usage: 38.2% (baseline usage), 50% and 80%. Compared to baseline usage of 38.2%, the result shows that scaling up the usage of LLINs to 50% in Kebbi State will reduce the incidence of malaria by 28.21%, while scaling up to the level of usage 80% will lead to a significant reduction of 78.93%. It is therefore recommended that, to bring down malaria incidence in Kebbi State to its bearest minimum, health policymakers in Nigeria should prioritise scaling up LLINs usage in the State by expanding LLIN distribution in the State and creating awareness on its proper usage.

However, the study is not without some limitations. Firstly, we have assumed a constant LLINs protective effectiveness rate and have not accounted for the decay rate of LLINs. This assumption in our model could lead to over-estimation of LLIN protective effectiveness in reducing malaria cases in the model predictions. Secondly, to reduce model complexity, the study did not explicitly account for the additional killing effect of LLINs. Thus, future studies should incorporate decay functions to capture the time-dependent loss of LLIN efficacy and the killing efficacy of LLIN to assess the impact of LLIN on regulating the mosquito population and mitigating further transmissions.

CRediT authorship contribution statement

Emmanuel A. Bakare: Investigation, Funding acquisition, Formal analysis, Data curation, Conceptualization. **Idowu I. Olasupo:** Methodology, Investigation, Formal analysis, Data curation. **Micheal Imoudu:** Project administration, Investigation, Formal analysis. **Afeez Abidemi:** Investigation, Formal analysis, Data curation. **Deborah O. Daniel:** Investigation, Formal analysis, Data curation. **Samuel A. Osikoya:** Investigation, Formal analysis, Data curation. **Oluwaseun A. Mogbojuri:** Investigation, Formal analysis, Data curation. **Aaron O. Nwana:** Investigation, Formal analysis. **Dolapo O. Oniyelu:** Investigation, Formal analysis, Conceptualization. **Ronke D. Olorunfemi:** Investigation, Formal analysis, Conceptualization. **Oluwafemi Samson Olagbami:** Investigation, Formal analysis. **Dorcas O. Agboola:** Project administration, Investigation, Formal analysis. **Steven I. Ikediashi:** Investigation, Formal analysis. **Ayomide Adedeji:** Investigation, Formal analysis, Conceptualization. **Oluwaponmile Ikuseka:** Project administration, Investigation, Formal analysis. **Micheal Fadairo:** Investigation, Formal analysis. **Odunayo Odewale:** Investigation, Formal analysis. **Ifeoma Goodness Onwuka:** Formal analysis, Data curation. **Aurel Hansinon:** Investigation, Formal analysis. **Dolapo A. Bakare:** Formal analysis, Data curation. **Lisa J. White:** Investigation, Formal analysis. **Nakul Chitnis:** Investigation, Formal analysis. **Olusola Oresanya:** Investigation. **Chukwu Okoronkwo:** Investigation, Data curation. **Eze Nelson:** Data curation. **Segun Kosoko:** Investigation, Formal analysis. **Gabriel I. Ogban:** Investigation, Formal analysis.

Code and data availability

The R codes used to generate the results presented in this manuscript are available from the corresponding author upon a reasonable request. Interested readers can reach out to the National Malaria Elimination Programme (NMEP), Nigeria, for the data used for this study.

Funding statement

This work was supported by a grant from the Gates Foundation (INV-047051). The funders had no role or influence on the design and interpretation of the data collected, as well as in writing the manuscript.

Declaration of competing interest

The authors declare that they have no known competing financial interests or personal relationships that could have appeared to influence the work reported in this paper.

Acknowledgments

The authors are grateful to the anonymous reviewers for their constructive comments, which have improved the quality of the original manuscript, and to NMEP and Malaria Consortium for their resourceful support.

A Qualitative analysis of the malaria model

In this appendix, we present the qualitative analysis of the autonomous version of the proposed malaria model by setting the seasonal-forcing mosquito biting rate $\epsilon(t) = \epsilon_0$.

A.1 Boundedness of solutions

Theorem A.1. *Let $N_h(t)$ and $N_m(t)$ represent the total human and mosquito populations in system* (10)*, respectively, which satisfies the differential equations:*

$$\frac{dN_h}{dt} = \Lambda_h - \mu_h N_h,$$
$$\frac{dN_m}{dt} = \Lambda_m - \mu_m N_m.$$

Then, the total populations $N_h(t)$ and$N_m(t)$ are uniformly bounded if:

i) $N_h(0) \leq \frac{\Lambda_h}{\mu_h}$, $N_m(0) \leq \frac{\Lambda_m}{\mu_m}$, *then* $N_h(t) \leq \frac{\Lambda_h}{\mu_h}$, $N_m(t) \leq \frac{\Lambda_m}{\mu_m}$ *for all time* $t > 0$;
ii) $N_h(0) \geq \frac{\Lambda_h}{\mu_h}$, $N_m(0) \leq \frac{\Lambda_m}{\mu_m}$, *then $N_h(t)$ and $N_m(t)$ asymptotically approach* $\frac{\Lambda_h}{\mu_h}$ *and* $\frac{\Lambda_m}{\mu_m}$, *respectively, as* $t \to \infty$.

Proof. The rate of change of the total human population is obtained by adding the right hand side of the first five equations in system (10):

$$\begin{aligned} \frac{dN_h}{dt} &= \Lambda_h - \mu_h N_h - \delta I_h, \\ &\leq \Lambda_h - \mu_h N_h. \end{aligned} \tag{11}$$

Integrating the inequality in (11) yields,

$$N_h(t) \leq \frac{\Lambda_h}{\mu_h}\left(1 - e^{-\mu_h t}\right) + N_0 e^{-\mu_h t},$$

so that, as $t \to \infty$, the human population is bounded by

$$N_h(t) \to \frac{\Lambda_h}{\mu_h}.$$

Similarly, the rate of change of the total mosquito population is obtained by adding the right-hand side of the last three equations in system (10) as

$$\frac{dN_m}{dt} = \Lambda_m - \mu_m N_m. \tag{12}$$

It follows from integrating the result in (12) that

$$N_m(t) \leq \frac{\Lambda_m}{\mu_m}\left(1 - e^{-\mu_m t}\right) + N_0 e^{-\mu_m t},$$

such that, as $t \to \infty$, the mosquito population is bounded by

$$N_m(t) \to \frac{\Lambda_m}{\mu_m}.$$

Since $\mu_h > 0$, if $N_h(0) \leq \frac{\Lambda_h}{\mu_h}$, then $N_h(t) \leq \frac{\Lambda_h}{\mu_h}$ for all $t > 0$. This proves that $N_h(t)$ is bounded above by $\frac{\Lambda_h}{\mu_h}$. Also, since $\mu_m > 0$, if $N_m(0) \leq \frac{\Lambda_m}{\mu_m}$, then $N_m(t) \leq \frac{\Lambda_m}{\mu_m}$ for all $t > 0$. This proves that $N_m(t)$ is bounded above by $\frac{\Lambda_m}{\mu_m}$. Therefore, both human, $N_h(t)$, and mosquito, $N_m(t)$, populations remain within biologically meaningful bounds. Hence, the proof.

A.2 Positivity of solutions

To ensure that the solutions remain biologically meaningful, we now prove that all state variables remain non-negative for all time $t > 0$.

Theorem A.2. *Suppose the initial values for the state variables are given by*

$$\Gamma(0) = \Big\{(S_h(0), E_h(0), I_h(0), A_h(0), S_m(0), E_m(0), I_m(0)) \in \mathbb{R}_+^4 \times \mathbb{R}_+^3 : S_h(0) > 0,\ E_h(0) \geq 0,$$
$$I_h(0) > 0,\ A_h(0) \geq 0, \geq 0, S_m(0) > 0,\ E_m(0) \geq 0,\ I_m(0) > 0\}$$

Then, the solutions of system (10) *satisfy*

$$\Gamma(t) = \Big\{(S_h(t), E_h(t), I_h(t), A_h(t), S_m(t), E_m(t), I_m(t)) \in \mathbb{R}_+^4 \times \mathbb{R}_+^3 : S_h(t) > 0, E_h(t) \geq 0,$$
$$I_h(t) \geq 0,\ A_h(t) \geq 0,\ \ S_m(t) > 0,\ E_m(t) \geq 0,\ I_m(t) \geq 0 \quad \text{for all} \ \ t \geq 0.$$

Proof. Considering the system in 10, we have

$$\frac{dS_h}{dt} = \Lambda_h + (\theta_I + u_2)I_h \geq -(\lambda_h(t) + \mu_h)S_h. \tag{13}$$

Integrating 13 gives

$$S_h(t) \geq S_h(0)\Big(- \int_0^t \lambda_h(t) + \mu_h \Big) dt > 0.$$

Similarly in system 10, it can be shown that, $E_h(t) > 0$, $I_h(t) > 0$, $A_h(t) > 0$, $S_m(t) > 0$, $E_m(t) > 0$, and $I_m(t) > 0$ for all $t > 0$.
We have shown that the solutions of the model are positive for all time $t > 0$ provided that the initial values of the state variables are non-negative. These results establish the biological feasibility of the model.

A.3 Disease free equilibrium point

The disease-free equilibrium point (DFE) occurs when the system reaches a steady state with no malaria infections (i.e., no infected individuals exist in the population). Specifically, the DFE of system (10) occurs when

$$\frac{dS_h}{dt} = \frac{dE_h}{dt} = \frac{dI_h}{dt} = \frac{dA_h}{dt} = \frac{dS_m}{dt} = \frac{dE_m}{dt} = \frac{dI_m}{dt} = 0,$$

with $E_h = I_h = A_h = E_m = I_m = 0$.
Now, from the first differential equation of model 10 at equilibrium, we have

$$\Lambda_h + (\theta_I + u_2)I_h^* - (\lambda_h(t) + \mu_h)S_h^* = 0. \tag{14}$$

Solving for S_h^* in 14 gives

$$S_h^* = \frac{\Lambda_h}{\mu_h}$$

Similarly, it is easy to obtain the equilibrium solution of the fifth equation of the malaria model (10) as

$$S_m^* = \frac{\Lambda_m}{\mu_m}.$$

Therefore, DEF of system 10 is obtained as

$$\mathcal{E}_0 = (S_h^*,\ E_h^*,\ I_h^*,\ A_h^*,\ S_m^*,\ E_m^*,\ I_m^*) = \left(\frac{\Lambda_h}{\mu_h},\ 0,\ 0,\ 0,\ \frac{\Lambda_m}{\mu_m},\ 0,\ 0\right).$$

A.4 Effective reproduction number

The effective reproduction number, denoted as $\mathcal{R}_e$, quantifies the potential for infection transmission in a population in the presence of interventions. Using the next-generation method, the van den Driessche and Watmough approach outlined in (van den Driessche & Watmough, 2002) is employed to compute the next-generation matrix related to model (10). The model is then written as $\frac{dx}{dt} = \mathcal{F}(x) - \mathcal{V}(x)$ where $\mathcal{F}$ represents the rate of appearance of new infections, and $\mathcal{V}$ describes the transfer of individuals in and out of the infected compartments.

Let the dynamics of the infected compartments (E_h, I_h, A_h, E_m, I_m) of model (10) be represented as

$$\dot{X} = \begin{pmatrix} \dot{E}_h \\ \dot{I}_h \\ \dot{A}_h \\ \dot{E}_m \\ \dot{I}_m \end{pmatrix}, \tag{15}$$

and the linearized system at the DFE takes the form

$$\dot{X} = (F - V)X.$$

Then, the rate of appearance of new infections in the population, f_i, is given by

$$\mathcal{F} = \begin{pmatrix} \frac{(1-u_1)\epsilon_0\beta_h S_h I_m}{N_h} \\ 0 \\ 0 \\ \frac{(1-u_1)\epsilon_0\beta_m S_m(\phi I_h + A_h)}{N_h} \\ 0 \end{pmatrix}, \tag{16}$$

while the rate of transfer of individuals in and out of the infected compartments, v_i, is given by

$$\mathcal{V} = \begin{pmatrix} m_3 E_h \\ -\rho\sigma_h E_h - \frac{\eta(1-u_1)\epsilon_0 A_h I_m}{N_h} + (m_1 + m_2) I_h \\ -(1-\rho)\sigma_h E_h + \mu_h A_h + \frac{\eta(1-u_1)\epsilon_0 A_h I_m}{N_h} \\ m_4 E_m \\ -\sigma_m E_m + \mu_m I_m \end{pmatrix}, \tag{17}$$

where $m_1 = \theta_I + u_2$, $m_2 = \delta + \mu_h$, $m_3 = \sigma_h + \mu_h$ and $m_4 = \sigma_m + \mu_m$. Hence, finding the Jacobian matrix of $\mathcal{F}$ in (16) and the Jacobian matrix of $\mathcal{V}$ in (17) at the DFE gives

$$F = \begin{pmatrix} 0 & 0 & 0 & 0 & (1-u_1)\epsilon_0\beta_h \\ 0 & 0 & 0 & 0 & 0 \\ 0 & 0 & 0 & 0 & 0 \\ 0 & \frac{(1-u_1)\epsilon_0\beta_m\phi\mu_h\Lambda_m}{\mu_m\Lambda_h} & \frac{(1-u_1)\epsilon_0\beta_m\mu_h\Lambda_m}{\mu_m\Lambda_h} & 0 & 0 \\ 0 & 0 & 0 & 0 & 0 \end{pmatrix}$$

and

$$V = \begin{pmatrix} m_3 & 0 & 0 & 0 & 0 \\ -\rho\sigma_h & m_1+m_2 & 0 & 0 & 0 \\ -(1-\rho)\sigma_h & 0 & \mu_h & 0 & 0 \\ 0 & 0 & 0 & m_4 & 0 \\ 0 & 0 & 0 & -\sigma_m & \mu_m \end{pmatrix}.$$

It follows that

$$V^{-1} = \begin{pmatrix} \frac{1}{m_3} & 0 & 0 & 0 & 0 \\ \frac{\rho\sigma_h}{m_3(m_1+m_2)} & \frac{1}{m_1+m_2} & 0 & 0 & 0 \\ \frac{(1-\rho)\sigma_h}{\mu_h m_3} & 0 & \frac{1}{\mu_h} & 0 & 0 \\ 0 & 0 & 0 & \frac{1}{m_4} & 0 \\ 0 & 0 & 0 & \frac{\sigma_m}{\mu_m m_4} & \frac{1}{\mu_m} \end{pmatrix}.$$

The next generation matrix FV^{-1} is obtained as

$$FV^{-1} = \begin{pmatrix} 0 & 0 & 0 & \frac{(1-u_1)\epsilon_0\beta_h\sigma_m}{m_4\mu_m} & \frac{(1-u_1)\epsilon_0\beta_h}{\mu_m} \\ 0 & 0 & 0 & 0 & 0 \\ 0 & 0 & 0 & 0 & 0 \\ \frac{(1-u_1)\epsilon_0\beta_m\Lambda_m\sigma_h[\phi\rho\mu_h+(1-\rho)(m_1+m_2)]}{\Lambda_h\mu_m(m_1+m_2)m_3} & \frac{(1-u_1)\epsilon_0\beta_m\phi\Lambda_m\mu_h}{\Lambda_h\mu_m(m_1+m_2)} & \frac{(1-u_1)\epsilon_0\beta_m\Lambda_m}{\Lambda_h\mu_m} & 0 & 0 \\ 0 & 0 & 0 & 0 & 0 \end{pmatrix}. \tag{18}$$

Therefore, the effective reproduction number of the malaria model (10) is the largest eigenvalue (also called the *spectral radius*) of FV^{-1} in (18), and is obtained as

$$\mathcal{R}_e = \sqrt{\frac{(1-u_1)^2\epsilon_0^2\beta_h\sigma_h[\phi\rho\mu_h+(1-\rho)(m_1+m_2)]\beta_m\sigma_m\Lambda_m}{\Lambda_h(m_1+m_2)m_3m_4\mu_m^2}}. \tag{19}$$

If $\mathcal{R}_e > 1$, the disease spread in the population which might lead to an outbreak or an epidemic. Also, if $\mathcal{R}_e < 1$, the infection will die out over time as each infected individual produces on average fewer than one new infection.

A.5 Local stability of disease free equilibrium

The existence of a disease-free equilibrium (DFE) has been established for the malaria model. To determine the long-term behavior of this equilibrium, we perform a stability analysis to assess whether the DFE is locally asymptotically stable or unstable.

Theorem A.3. *The malaria disease-free equilibrium state of the model is locally asymptotically stable when $\mathcal{R}_e < 1$ and unstable when $\mathcal{R}_e > 1$.*

Proof. Jacobian matrix of model (10) at DFE is given by

$$J=\begin{pmatrix} -\mu_h & 0 & m_1 & 0 & 0 & 0 & -(1-u_1)\epsilon_0\beta_h \\ 0 & -m_3 & 0 & 0 & 0 & 0 & (1-u_1)\epsilon_0\beta_h \\ 0 & \rho\sigma_h & -(m_1+m_2) & 0 & 0 & 0 & 0 \\ 0 & (1-\rho)\sigma_h & 0 & -\mu_h & 0 & 0 & 0 \\ 0 & 0 & -\dfrac{(1-u_1)\epsilon_0\beta_m\Lambda_m\phi\mu_h}{\mu_m\Lambda_h} & -\dfrac{(1-u_1)\epsilon_0\beta_m\Lambda_m\mu_h}{\mu_m\Lambda_h} & -\mu_m & 0 & 0 \\ 0 & 0 & \dfrac{(1-u_1)\epsilon_0\beta_m\phi\mu_h\Lambda_m}{\Lambda_h\mu_m} & \dfrac{(1-u_1)\epsilon_0\beta_m\mu_h\Lambda_m}{\Lambda_h\mu_m} & 0 & -m_4 & 0 \\ 0 & 0 & 0 & 0 & 0 & \sigma_m & -\mu_m \end{pmatrix}. \tag{20}$$

The Jacobian matrix (20) provides seven eigenvalues, which include $-\mu_h$ and $-\mu_m$. The remaining eigenvalues are the roots of the characteristic equation

$$\lambda^5 + a_1\lambda^4 + a_2\lambda^3 + a_3\lambda^2 + a_4\lambda^1 + a_5 = 0, \tag{21}$$

where

$$\begin{aligned} a_1 &= m_1 + m_2 + m_3 + m_4 + \mu_h + \mu_m, \\ a_2 &= (m_1 + m_2 + m_3 + m_4)(\mu_h + \mu_m) + (m_1 + m_2)(m_3 + m_4) + m_3m_4 + \mu_h\mu_m, \\ a_3 &= m_3(m_1 + m_2)(m_4 + \mu_h + \mu_m) + m_4(m_1 + m_2 + m_3)(\mu_h + \mu_m) + \mu_h\mu_m(m_1 + m_2 + m_3 + m_4), \\ a_4 &= m_3m_4(m_1 + m_2)(\mu_h + \mu_m) + m_1\mu_h\mu_m(m_3 + m_4) + \mu_h\mu_m[m_2(m_3 + m_4) + m_3m_4] \\ &\quad - \frac{(1-u_1)^2\epsilon_0^2\beta_h\mu_h\sigma_h[\phi\rho + (1-\rho)]\beta_m\sigma_m\Lambda_m}{\Lambda_h\mu_m}, \\ a_5 &= (m_1 + m_2)m_3m_4\mu_h\mu_m\left(1 - \mathcal{R}_e^2\right). \end{aligned}$$

By the Routh-Hurwitz criteria in (Kim et al., 2018), the polynomial in (21) has negative real roots provided that $a_1 > 0$, $a_2 > 0$, $a_3 > 0$, $a_4 > 0$, $a_5 > 0$, $a_1a_2a_3 > a_1^2a_4 + a_3^2$ and $(a_1a_4 - a_5)(a_1a_2a_3 - a_3^2 - a_1^2a_4) > a_5(a_1a_2 - a_3)^2 + a_1a_5^2$ along with the condition $\mathcal{R}_e < 1$. It implies that, with negative real eigenvalues, the disease-free equilibrium state is locally asymptotically stable.

A.6 Endemic equilibrium point of model (10)

At the endemic equilibrium, the infection persists in the population, so $E_h, A_h, I_h, E_m, I_m \neq 0$ in the malaria model (10). Let the endemic equilibrium of the model be given by

$$\mathcal{E}_1 = (S_h^{**}, E_h^{**}, I_h^{**}, A_h^{**}, S_m^{**}, E_m^{**}, I_m^{**}). \tag{22}$$

Further, let the forces of infection in human and mosquito at steady state be defined as

$$\lambda_h^{**} = \frac{(1-u_1)\epsilon_0\beta_h I_m^{**}}{N_h^{**}} \quad \text{and} \quad \lambda_m^{**} = \frac{(1-u_1)\epsilon_0\beta_m\left(\phi I_h^{**} + A_h^{**}\right)}{N_h^{**}}. \tag{23}$$

Thus, solving system (10) at steady state in terms of the forces of infection in (23) gives the components of $\mathcal{E}_1$ in (22) as

$$
\begin{aligned}
S_h^{**} &= \frac{\Lambda_h(m_1+m_2)m_3\left(\eta\lambda_h^{**}+\mu_h\right)}{\eta[(m_1+m_2)m_3-m_1\sigma_h](\lambda^{**})^2+\mu_h[(m_1+m_2)m_3(\eta+1)-m_1\sigma_h\rho]\lambda_h^{**}+(m_1+m_2)m_3\mu_h^2},\\
E_h^{**} &= \frac{\lambda_h^{**}}{m_3}S_h^{**},\\
I_h^{**} &= \frac{\left(\eta\lambda_h^{**}+\rho\mu_h\right)\sigma_h\lambda_h^{**}}{(m_1+m_2)m_3\left(\eta\lambda_h^{**}+\mu_h\right)}S_h^{**},\\
A_h^{**} &= \frac{(1-\rho)\sigma_h\lambda_h^{**}}{m_3\left(\eta\lambda_h^{**}+\mu_h\right)}S_h^{**},\\
S_m^{**} &= \frac{\Lambda_m}{\lambda_m^{**}+\mu_m},\\
E_m^{**} &= \frac{\Lambda_m\lambda_m^{**}}{m_4\left(\lambda_m^{**}+\mu_m\right)},\\
I_m^{**} &= \frac{\sigma_m\Lambda_m\lambda_m^{**}**}{\mu_m m_4\left(\lambda_m^{**}+\mu_m\right)}.
\end{aligned}
\tag{24}
$$

Substituting the appropriate results in (24) into the forces of infection in (23) and simplifying give rise to the following polynomial equation:

$$
f(\lambda^{**}) := b_0+b_1\lambda_h^{**}+b_2\left(\lambda_h^{**}\right)^2+b_3\left(\lambda_h^{**}\right)^3+b_4\left(\lambda_h^{**}\right)^4=0,
\tag{25}
$$

where

$$
\begin{aligned}
b_4 &= \Lambda_h m_4\mu_m\eta(m_1+m_2+\sigma_h)[(1-u_1)\epsilon_0\beta_m\sigma_h\phi+\mu_m(m_1+m_2+\sigma_h)],\\
b_3 &= \Lambda_h m_4\mu_m\{[(m_1+m_2)[m_3\eta+\mu_h+\sigma_h(1-\rho)]+\sigma_h\rho\mu_h]\eta[(1-u_1)\epsilon_0\beta_m\sigma_h\phi\\
&\quad+\mu_m(m_1+m_2+\sigma_h)]+\eta(m_1+m_2+\sigma_h)\{(1-u_1)\epsilon_0\beta_m\sigma_h[\phi\mu_h+(1-\rho)(m_1+m_2)]\\
&\quad+(m_1+m_2)[m_3\eta+\mu_h+\sigma_h(1-\rho)]+\sigma_h\rho\mu_h\}\}\\
&\quad-(1-u_1)^2\epsilon_0^2\beta_h\sigma_h\beta_m\sigma_m\phi\eta^2\Lambda_m[(m_1+m_2)m_3-m_1\sigma_h],\\
b_2 &= \Lambda_h m_4\mu_m\{(m_1+m_2)m_3\mu_h\eta[(1-u_1)\epsilon_0\beta_m\sigma_h\phi+\mu_m(m_1+m_2+\sigma_h)]\\
&\quad[(m_1+m_2)[m_3\eta+\mu_h+\sigma_h(1-\rho)]+\sigma_h\rho\mu_h]\\
&\quad\times\{(1-u_1)\epsilon\beta_m\sigma_h[\phi\mu_h+(1-\rho)(m_1+m_2)]\\
&\quad+(m_1+m_2)[m_3\eta+\mu_h+\sigma_h(1-\rho)]+\sigma_h\rho\mu_h\}\\
&\quad+\mu_m(m_1+m_2)m_3\mu_h\eta(m_1+m_2+\sigma_h)\}\\
&\quad-(1-u_1)^2\epsilon_0^2\beta_h\sigma_h\beta_m\sigma_m\eta\mu_h\Lambda_m\{\phi[(m_1+m_2)m_3(\eta+1)-m_1\sigma_h\rho]\\
&\quad+[\phi\rho\mu_h+(1-\rho)(m_1+m_2)][(m_1+m_2)m_3-m_1\sigma_h]\},\\
b_1 &= \Lambda_h m_4\mu_m\{m_3\mu_h(m_1+m_2)\{(1-u_1)\epsilon_0\beta_m\sigma_h[\phi+\mu_h+(1-\rho)(m_1+m_2)]\\
&\quad+(m_1+m_2)[m_3\eta+\mu_h+\sigma_h(1-\rho)]+\sigma_h\rho\mu_h\}\\
&\quad+\mu_h\mu_m m_3(m_1+m_2)[(m_1+m_2)[m_3\eta+\mu_h+\sigma_h(1-\rho)]+\sigma_h\rho\mu_h]\}\\
&\quad-(1-u_1)^2\epsilon_0^2\beta_h\sigma_h\beta_m\sigma_m\mu_h\Lambda_m\{\phi\eta(m_1+m_2)m_3\mu_h+[\phi\rho\mu_h+(1-\rho)(m_1+m_2)]\\
&\quad\times[(m_1+m_2)m_3(\eta+1)-m_1\sigma_h\rho]\},\\
b_0 &= \Lambda_h\mu_h^2\mu_m^2(m_1+m_2)^2m_3^2m_4\left(1-\mathcal{R}_e^2\right).
\end{aligned}
$$

Solving for λ_h^{**} in (25) consequently leads to obtaining the positive endemic equilibrium $\mathcal{E}_1$ of the malaria model (10). Since the model parameters are non-negative, $b_4 > 0$ always holds, whereas $b_0 > 0$ ($b_0 < 0$) whenever $\mathcal{R}_e < 1$ ($\mathcal{R}_e > 1$). Thus, the number of possible positive real roots of polynomial (25) is determined by the signs of the coefficients b_1, b_2 and b_3. Solving (25) for the positive values of λ_h^{**} allows us to explicitly determine the positive endemic equilibria of the malaria model (10). By Descartes' rule of signs (see Theorem 4.10 in (Elwyn Meserve, 1982)), the summary of the various possibilities for the positive roots of the polynomial whenever $\mathcal{R}_e < 1$ and $\mathcal{R}_e > 1$ are displayed in Table 7.

Table 7
Different cases and their corresponding total number of possible real roots of polynomial (25)

Case	Coefficient of polynomial (25)					$\mathcal{R}_e$	Number of sign changes	Number of possible positive real roots
	b_0	b_1	b_2	b_3	b_4			
I	+	+	+	+	+	<1	0	0
II	−	−	+	+	+	>1	1	1
III	+	+	−	+	+	<1	2	0, 2
IV	−	+	+	−	+	>1	3	1, 3
V	+	−	+	−	+	<1	4	0, 2, 4

It should be mentioned that all the other possible sign changes such that Cases II, III and IV hold are omitted in Table 7. Consequently, the results in the table give birth to the following Theorem:

Theorem A.4. *The model of malaria transmission dynamics and control* (10) *admits:*

i. *Only one (unique) endemic equilibrium when case II in* Table 7 *is applicable and* $\mathcal{R}_e > 1$;
ii. *More than one endemic equilibrium when case IV in* Table 7 *is applicable and* $\mathcal{R}_e > 1$;
iii. *More than one endemic equilibrium if cases III and V in* Table 7 *are applicable such that* $\mathcal{R}_e < 1$;
iv. *No endemic equilibrium otherwise, whenever case I in* Table 7 *holds and* $\mathcal{R}_e < 1$.

Remark A.1. *Condition iii of Theorem A.4 indicates the potential for the occurrence of a backward bifurcation,* characterised by the coexistence of a stable disease-free equilibrium and a stable endemic equilibrium when $\mathcal{R}_e < 1$. However, the investigation of this backward bifurcation phenomenon is beyond the scope of the present study and is therefore not pursued further.

A.7 Sensitivity analysis

In this part of the paper, the focus is on examining how the model parameters influence the transmission dynamics and control of *Plasmodium falciparum* malaria in the interacting human and mosquito populations. This paper considers local sensitivity analysis. In that case, the sensitivity indices of the effective reproduction number, $\mathcal{R}_e$, with respect to the model parameters are obtained using the normalized forward-sensitivity index defined by

$$\Theta_p^{\mathcal{R}_e} = \frac{p}{\mathcal{R}_e}\frac{\partial \mathcal{R}_e}{\partial p}, \tag{26}$$

where p is any parameter contained in the expression for $\mathcal{R}_e$ in (19). Thus, we are led to the following analytical sensitivity indices:

$$
\begin{aligned}
\Theta_{\epsilon_0}^{\mathcal{R}_e} &= \frac{\epsilon_0}{\mathcal{R}_e}\frac{\partial \mathcal{R}_e}{\partial \epsilon_0} = +1,\\
\Theta_{\beta_h}^{\mathcal{R}_e} &= \frac{\beta_h}{\mathcal{R}_e}\frac{\partial \mathcal{R}_e}{\partial \beta_h} = +\frac{1}{2},\\
\Theta_{\mu_h}^{\mathcal{R}_e} &= \frac{\mu_h}{\mathcal{R}_e}\frac{\partial \mathcal{R}_e}{\partial \mu_h} = -\frac{1}{2}\frac{\mu_h\left[(1-\rho)(\delta+\mu_h+\theta_I+u_2)^2-\phi\rho\left(\delta\sigma_h-\mu_h^2+\sigma_h\theta_I+\sigma_h u_2\right)\right]}{(\delta+\mu_h+\theta_I+u_2)(\sigma_h+\mu_h)[\phi\rho\mu_h+(1-\rho)(\delta+\mu_h+\theta_I+u_2)]},\\
\Theta_{\sigma_h}^{\mathcal{R}_e} &= \frac{\sigma_h}{\mathcal{R}_e}\frac{\partial \mathcal{R}_e}{\partial \sigma_h} = +\frac{1}{2}\frac{\mu_h}{\sigma_h+\mu_h},\\
\Theta_{\phi}^{\mathcal{R}_e} &= \frac{\phi}{\mathcal{R}_e}\frac{\partial \mathcal{R}_e}{\partial \phi} = +\frac{1}{2}\frac{\phi\rho\mu_h}{\phi\rho\mu_h+(1-\rho)(\delta+\mu_h+\theta_I+u_2)},\\
\Theta_{\rho}^{\mathcal{R}_e} &= \frac{\rho}{\mathcal{R}_e}\frac{\partial \mathcal{R}_e}{\partial \rho} = +\frac{1}{2}\frac{\rho\phi\mu_h}{\phi\rho\mu_h+(1-\rho)(\delta+\mu_h+\theta_I+u_2)},\\
\Theta_{\theta_I}^{\mathcal{R}_e} &= \frac{\theta_I}{\mathcal{R}_e}\frac{\partial \mathcal{R}_e}{\partial \theta_I} = -\frac{1}{2}\frac{\phi\rho\theta_I\mu_h}{(\delta+\mu_h+\theta_I+u_2)[\phi\rho\mu_h+(1-\rho)(\delta+\mu_h+\theta_I+u_2)]},\\
\Theta_{\delta}^{\mathcal{R}_e} &= \frac{\delta}{\mathcal{R}_e}\frac{\partial \mathcal{R}_e}{\partial \delta} = -\frac{1}{2}\frac{\phi\rho\delta\mu_h}{(\delta+\mu_h+\theta_I+u_2)[\phi\rho\mu_h+(1-\rho)(\delta+\mu_h+\theta_I+u_2)]},\\
\Theta_{\beta_m}^{\mathcal{R}_e} &= \frac{\beta_m}{\mathcal{R}_e}\frac{\partial \mathcal{R}_e}{\partial \beta_m} = +\frac{1}{2},\\
\Theta_{\sigma_m}^{\mathcal{R}_e} &= \frac{\sigma_m}{\mathcal{R}_e}\frac{\partial \mathcal{R}_e}{\partial \sigma_m} = +\frac{1}{2}\frac{\mu_m}{\sigma_m+\mu_m},\\
\Theta_{\Lambda_m}^{\mathcal{R}_e} &= \frac{\Lambda_m}{\mathcal{R}_e}\frac{\partial \mathcal{R}_e}{\partial \Lambda_m} = +\frac{1}{2},\\
\Theta_{\Lambda_h}^{\mathcal{R}_e} &= \frac{\Lambda_h}{\mathcal{R}_e}\frac{\partial \mathcal{R}_e}{\partial \Lambda_h} = -\frac{1}{2},\\
\Theta_{\mu_m}^{\mathcal{R}_e} &= \frac{\mu_m}{\mathcal{R}_e}\frac{\partial \mathcal{R}_e}{\partial \mu_m} = -\frac{1}{2}\frac{2\sigma_m+3\mu_m}{\sigma_m+\mu_m},\\
\Theta_{u_1}^{\mathcal{R}_e} &= \frac{u_1}{\mathcal{R}_e}\frac{\partial \mathcal{R}_e}{\partial u_1} = -\frac{u_1}{1-u_1},\\
\Theta_{u_2}^{\mathcal{R}_e} &= \frac{u_2}{\mathcal{R}_e}\frac{\partial \mathcal{R}_e}{\partial u_2} = -\frac{1}{2}\frac{\phi\rho u_2\mu_h}{(\delta+\mu_h+\theta_I+u_2)[\phi\rho\mu_h+(1-\rho)(\delta+\mu_h+\theta_I+u_2)]}.
\end{aligned}
$$

All the analytical indices derived, as presented above, are quantified in section 3.

References

Abubakar Saleh, J.-E., Saddiq, A., & Uchenna, A. A. (2018). LLIN ownership, utilization, and malaria prevalence: An outlook at the 2015 Nigeria malaria indicator survey. *Open Access Library Journal, 5*(1), 1–3.

Adegbenro, W., Oni, E. T., Oba-Ado, O., Folayan, W. A., Olafimihan, M. O., Arowolo, T., & Afolabi, B. M. (2018). Replacement campaign of long lasting insecticide treated nets in ondo state, southwest Nigeria, heartland of africa's most efficient vector species. *Diversity and Equality in Health and Care, 15*(3), 95–103.

Ahu Prah, D., & Laryea-Akrong, E. (2024). Asymptomatic low-density plasmodium falciparum infections: Parasites under the host's immune radar? *The Journal of Infectious Diseases, 229*(6), 1913–1918.

Aliyu Abdulkarim, I., Ibrahim Yakudima, I., Abdullahi, J. G., & Adamu, Y. M. (2023). Geographical analysis of malaria in nigeria–spatiotemporal patterns of national and subnational incidence. In *Health and medical geography in Africa: Methods, applications and development linkages* (pp. 185–209). Springer.

Babalola, O. J., Sambo, M. N., Idris, S. H., Ajayi, I.-O. O., Ajumobi, O., & Nguku, P. (2019). Factors associated with utilization of llins among women of child-bearing age in igabi, kaduna state, Nigeria. *Malaria Journal, 18*(1), 412.

Bakare, E. A., Bayode Are, E., Abolarin, O. E., Ayodeji Osanyinlusi, S., Ngwu, B., & Ubaka, O. N. (2020). Mathematical modelling and analysis of transmission dynamics of lassa fever. *Journal of Applied Mathematics, 2020*(1), Article 6131708.

Bakare, E. A., Onasanya, B. O., Hoskova-Mayerova, S., & Olubosede, O. (2021). Analysis of control interventions against malaria in communities with limited resources. *Analele ştiinţifice ale Universităţii" Ovidius" Constanţa. Seria Matematică, 29*(2), 71–91.

Bhattarai, A., Ali, A. S., Kachur, S. P., Mårtensson, A., Abbas, A. K., Rashid, K., Al-Mafazy, A. Wahiyd, Ramsan, M., Rotllant, G., Gerstenmaier, J. F., et al. (2007). Impact of artemisinin-based combination therapy and insecticide-treated nets on malaria burden in zanzibar. *PLoS Medicine, 4*(11), Article e309.

CDC. (2024). About malaria. URL https://www.cdc.gov/malaria/about/index.html. (Accessed 28 September 2024).

Chitnis, N., Hyman, J. M., & Cushing, J. M. (2008). Determining important parameters in the spread of malaria through the sensitivity analysis of a mathematical model. *Bulletin of Mathematical Biology, 70*, 1272–1296.

Coetzee, M. (2020). Key to the females of afrotropical anopheles mosquitoes (diptera: Culicidae). *Malaria Journal, 19*, 1–20.

Dako-Gyeke, P., Asampong, E., Glozah, F. N., Hornuvo, R., Teg-Nefaah Tabong, P., Gittelman, D., Nwameme, A., Oteng, B., Peprah, N. Y., Chandi, G. M., et al. (2024). Assessing llin distribution implementation using evidence-informed intervention core elements: A qualitative study in a resource-constrained setting. *BMC Health Services Research, 24*(1), 790.

Elwyn Meserve, B. (1982). Fundamental concepts of algebra. *Courier Corporation*.
Federal ministry of health. (2022). Federal ministry of health, national malaria elimination programme (nmep). URL https://www.health.gov.ng/index.phpption=com_content&view=article&id=328&Itemid=550.
Gimba, B., & Bala, S. I. (2017). Modeling the impact of bed-net use and treatment on malaria transmission dynamics. *Int. Sch. Res. Notices*, Article 6182492.
Idris, U. B. (2023). *Assessment of the implementation of demographic aspect of the nigeria's national population policy in Kebbi state, Nigeria*.
Kim, J.-H., Su, W., & Song, Y. J. (2018). On stability of a polynomial. *Journal of Applied Mathematics Informatics, 36*(3-4), 231–236.
Kumar, R., Farzeen, M., Hafeez, A., Achakzai, B. K., Vankwani, M., Lal, M., & Somrongthong, R. (2020). Effectiveness of a health education intervention on the use of long-lasting insecticidal nets for the prevention of malaria in pregnant women of Pakistan: A quasi-experimental study. *Malaria Journal, 19*, 1–10.
Kusimo, N. O., Matthew, D. E., Olasunkanmi, B. A., Agwae, M. E., & Kusimo, M. O. (2019). Understanding the importance of malaria control tools by pregnant and nursing mothers is key to ending malaria burden in Nigeria: A case study of eight communities in south-south Nigeria. *International NGO Journal, 14*(5), 64–69.
Legates, D. R., & McCabe, G. J., Jr. (1999). Evaluating the use of "goodness-of-fit" measures in hydrologic and hydroclimatic model validation. *Water Resources Research, 35*(1), 233–241.
Lindblade, K. A., Steinhardt, L., Samuels, A., Kachur, S. P., & Slutsker, L. (2013). The silent threat: Asymptomatic parasitemia and malaria transmission. *Expert Review of Anti-infective Therapy, 11*(6), 623–639.
Mamoudou, S. (2021). Economic and political factor of Songhay empire the emergence of Kebbi kingdom Nigeria, c. 1500s. *Open Journal of Social Sciences, 9*(4), 332–345.
Mandala, W. L., Harawa, V., Dzinjalamala, F., & Tembo, D. (2021). The role of different components of the immune system against plasmodium falciparum malaria: Possible contribution towards malaria vaccine development. *Molecular and Biochemical Parasitology, 246*, Article 111425.
Mehta, J. (2024). *Optimizing malaria control in Nigeria: A comprehensive review of llin effectiveness and policy frameworks*.
Mosha, J. F., Kulkarni, M. A., Lukole, E., Matowo, N. S., Pitt, C., Messenger, L. A., & Protopopoff, N. (2022). Effectiveness and cost-effectiveness against malaria of three types of dual-active-ingredient long-lasting insecticidal nets (llins) compared with pyrethroid-only llins in Tanzania: A four-arm, cluster-randomised trial. *The Lancet, 399*(10331), 1227–1241.
Mukhtar, A. Y. A., Munyakazi, J. B., Ouifki, R., & Clark, A. E. (2018). Modelling the effect of bednet coverage on malaria transmission in South Sudan. *PLoS One, 13*(6), Article e0198280.
National Malaria Data Repository. National malaria data repository. https://nmdrnigeria.ng/dhis-web-commons/security/login.action,2025. (Accessed 22 May 2025). Contact:nmdrhelpdesk@nmep.gov.ng.
National Malaria Elimination Programme (NMEP). (2021a). *Nigeria malaria indicator survey 2021 final report, National Malaria Elimination Programme (NMEP)*.
National Malaria Elimination Programme (NMEP). (2021b). Nigeria malaria strategic plan 2021-2025, National Malaria Elimination Programme (NMEP). URL https://nmcp.gov.ng/. (Accessed 10 February 2025).
National population commission. (2018). *Nigeria demographic health survey (dhs)*. abuja, nigeria. URL https://www.dhsprogram.com/pubs/pdf/MIS20.pdf.
Ngonghala, C. N. (2022). Assessing the impact of insecticide-treated nets in the face of insecticide resistance on malaria control. *Journal of Theoretical Biology, 555*, Article 111281.
Ngonghala, C. N., Del Valle, S. Y., Zhao, R., & Mohammed-Awel, J. (2014). Quantifying the impact of decay in bed-net efficacy on malaria transmission. *Journal of Theoretical Biology, 363*, 247–261.
Obi, E., Okoh, F., Blaufuss, S., Olapeju, B., Akilah, J., Okoko, O. O., Okechukwu, A., Maire, M., Popoola, K., Yahaya, M. A., et al. (2020). Monitoring the physical and insecticidal durability of the long-lasting insecticidal net dawaplus® 2.0 in three states in Nigeria. *Malaria Journal, 19*, 1–19.
Ojurongbe, O., Lawal, O. A., Abiodun, O. O., Okeniyi, J. A., Oyeniyi, A. J., & Oyelami, O. A. (2013). Efficacy of artemisinin combination therapy for the treatment of uncomplicated falciparum malaria in Nigerian children. *Journal of Infection in Developing Countries, 7*(12), 975–982.
Okell, L. C., Drakeley, C. J., Bousema, T., Whitty, C. J. M., & Ghani, A. C. (2008). Modelling the impact of artemisinin combination therapy and long-acting treatments on malaria transmission intensity. *PLoS Medicine, 5*(11), Article e226.
Portugal, S., Tran, T. M., Ongoiba, A., Bathily, A., Li, S., Doumbo, S., Skinner, J., Doumtabe, D., Kone, Y., Sangala, J., et al. (2017). Treatment of chronic asymptomatic plasmodium falciparum infection does not increase the risk of clinical malaria upon reinfection. *Clinical Infectious Diseases, 64*(5), 645–653.
Richards, F. O., Emukah, E., Graves, P. M., Nkwocha, O., Nwankwo, L., Rakers, L., Mosher, A., Patterson, A., Ozaki, M., Nwoke, B. E. B., et al. (2013). Community-wide distribution of long-lasting insecticidal nets can halt transmission of lymphatic filariasis in southeastern Nigeria. *The American Journal of Tropical Medicine and Hygiene, 89*(3), 578.
UNICEF. (2022). *Fighting malaria with long-lasting insecticidal nets (llins)*.
van den Driessche, P., & Watmough, J. (2002). Reproduction numbers and sub-threshold endemic equilibria for compartmental models of disease transmission. *Mathematical Biosciences, 180*(1–2), 29–48.
Viana, M., Hughes, A., Matthiopoulos, J., Ranson, H., & Ferguson, H. M. (2016). Delayed mortality effects cut the malaria transmission potential of insecticide-resistant mosquitoes. *Proceedings of the National Academy of Sciences, 113*(32), 8975–8980.
Wali, S., Gada, M., Hamisu, I., Umar, K. J., & Abor, I. G. (2022). Evaluation of shallow groundwater in rural Kebbi state, nw Nigeria, using multivariate analysis: Implication for grou ndwater quality management. *MOJ Eco Environment Science, 7*(3), 65–75.
WHO. Fact sheet about malaria. https://www.who.int/news-room/fact-sheets/detail/malaria. (Accessed 11 February 2025).
WHO. (2005). *Guidelines for laboratory and field testing of long-lasting insecticidal mosquito nets*.
Willmott, C. J. (1981). On the validation of models. *Physical Geography, 2*(2), 184–194. https://doi.org/10.1080/02723646.1981.10642213
World Health Organization. (2010). Mathematical modelling to support malaria control and elimination. https://iris.who.int/bitstream/handle/10665/87051/9789241500418_eng.pdf?sequence=1. (Accessed 17 February 2025).
World Health Organization. (2017). Who recommendations for achieving universal coverage with long-lasting insecticidal nets in malaria control. URL https://www.who.int/docs/default-source/malaria/mpac-documentation/mpac-oct2017-draft-updated-recommendations-universal-llin-coverage-session9.pdf.
World health organization. (2021). *World Malaria report 2021*. World Health Organization. URL https://www.who.int/teams/global-malaria-programme/reports/world-malaria-report-2021.
World Health Organization. (2023). *World malaria report 2023*. World Health Organization.
World Health Organization Regional Office for Africa. (2023). *Report on malaria in Nigeria 2022*. Licence: CC BY-NC-SA 3.0 IGO.
World Health Organization (WHO) Africa. Protecting families against malaria using long-lasting insecticide nets, n.d. URL https://www.afro.who.int/countries/nigeria/news/protecting-families-against-malaria-using-long-lasting-insecticide-nets. Accessed: 2025-February-16.
Wubishet, M. K., Berhe, G., Adissu, A., & Tafa, M. S. (2021). Effectiveness of long-lasting insecticidal nets in prevention of malaria among individuals visiting health centres in ziway-dugda district, Ethiopia: Matched case–control study. *Malaria Journal, 20*(1), 301.
Zayyanu Magawata, U., & Yahaya, A. A. (2019). Trends and variations of monthly solar radiation, temperature and rainfall data over birnin Kebbi metropolis for the period of 2014-2016. *Journal of Geography, Environment and Earth Science International, 21*(2), 1–10.
Zhang, X., & Deitsch, K. W. (2022). The mystery of persistent, asymptomatic plasmodium falciparum infections. *Current Opinion in Microbiology, 70*, Article 102231.